SKB

TECHNICAL REPORT 88-11

Groundwater numerical modelling of the Fjällveden study site – Evaluation of parameter variations
A HYDROCOIN study – Level 3, case 5A

Nils-Åke Larsson[1], Anders Markström[2]

[1] Swedish Geological Company, Uppsala
[2] Kemakta Consultants Co, Stockholm

October 1987

SVENSK KÄRNBRÄNSLEHANTERING AB
SWEDISH NUCLEAR FUEL AND WASTE MANAGEMENT CO

BOX 5864 S-102 48 STOCKHOLM
TEL 08-665 28 00 TELEX 13108-SKB

GROUNDWATER NUMERICAL MODELLING OF THE FJÄLLVEDEN STUDY SITE - EVALUATION OF PARAMETER VARIATIONS

A HYDROCOIN STUDY - LEVEL 3, CASE 5A

Nils-Åke Larsson[1], Anders Markström[2]

1 Swedish Geological Company, Uppsala
2 Kemakta Consultants Co, Stockholm

October 1987

SWEDISH GEOLOGICAL COMPANY
Division of Engineering Geology
Client: SKB

REPORT
ID-no: IRAP 87388
Date: 1987-10-01

GROUNDWATER NUMERICAL MODELLING OF THE FJÄLLVEDEN STUDY SITE - EVALUATION OF PARAMETER VARIATIONS

A HYDROCOIN STUDY - LEVEL 3, CASE 5A

Nils-Åke Larsson[1]
Anders Markström[2]

[1] Swedish Geological Company, Uppsala
[2] Kemakta Konsult AB, Stockholm

ABSTRACT

Level 3 of the Hydrocoin project concerns the sensitivity and uncertainty analysis of groundwater flow calculations. In the present study the sensitivity/uncertainty of the hydraulic conductivity distribution in crystalline rocks is considered at the Fjällveden study site - a site included in the Swedish site selection programme for final storage of spent nuclear fuel. A three-dimensional FEM-model assuming steady-state flow with constant fluid properties under saturated conditions is used.

The bedrock of the site is divided into three hydraulic units; rock mass, local and regional fracture zones. The data set of hydraulic conductivity of each unit has been treated statistically in various ways, reflecting different aspects of the physical conditions of the site. A total of nine cases have been prepared, all based on 214 data points.

The calculated head distribution and flow pattern for the model cases differ very little, while the flow rates and residence times vary more significantly (2-3 times).

The results of each parameter analysed separate the model cases as expected; a hydraulic contrast between rock mass and fracture zones enhances the hydraulic gradient and flow rate, and decreases the quality of the numerical solution. Anisotropic hydraulic conductivity in the rock mass skewes the head isopotentials to be more parallel with the main direction of the anisotropy, etc. However, the combined effect illustrated by the particle trajectories and residence times is not that easy to predict. The effect of anisotropy becomes significant at depths greater than approx. 300-500 m as the head gradient from the groundwater table is flattened out.

Groundwater recharge as a measure of quality assurance of the model calculations at repository depth is of limited use as it primarily reflects the hydraulic conditions in the surficial bedrock.

Finally, for more site specific modelling in the future computers of greater capacity has to be used to overcome simplifications in the discretisation of the conceptual model.

GROUNDWATER NUMERICAL MODELLING OF THE FJÄLLVEDEN STUDY SITE
- EVALUATION OF PARAMETER VARIATIONS - A HYDROCOIN STUDY -
LEVEL 3, CASE 5A

1. INTRODUCTION

The Swedish Power Inspectorate (SKI) initiated an international project called HYDROCOIN (May 1984) in order to test the accuracy and applicability of computer codes designated to simulate ground water flow. The study is divided in three levels aiming at:

Level 1 Verification of computer codes for groundwater calculations

Level 2 Validation of mathematical models for groundwater flow

Level 3 Sensitivity and uncertainty analysis of groundwater flow calculations

Level 1 is performed by comparing calculated results with analytical solutions and intercomparing results from different numerical programs. Totally seven test cases have been tackled at Level 1.

Level 2 involves the numerical solution of field and laboratory experiments . Five test cases have been decided to form basis for Level 2.

This report concerns Case 5A within Level 3 of the HYDROCOIN study carried out on behalf of the Swedish Nuclear Fuel and Waste Management Co (SKB). Case 5A adresses the issue of uncertainty analysis of flow problems in crystalline rock. The case is based on the field situation at the Swedish Fjällveden study site which has previously been evaluated as part of the KBS 3-study, Ahlbom et al (1983a), Carlsson et al (1983), SKBF (1983).

In the test-case three sources of uncertainty were suggested to be investigated:

- Boundary conditions

- Permeability distribution

- Numerical model

However, in this paper foremost the sensitivity/uncertainty of the spatial distribution of the hydraulic conductivity in the bedrock is considered.

2. DESCRIPTION OF PHYSICAL CASES

2.1 The Fjällveden study site

In the current report the main characteristics of the study site are presented. A more thorough description of the site and the investigation methods is given by Ahlbom et al, 1983a and b.

The site is located between two regional lineaments that are separated some 3 km apart. The investigated area comprises approximately 4 km^2. Based on data from geological, geophysical and hydrogeological investigations the bedrock within the site is divided into different hydraulic units including regional fracture zones, local fracture zones and rock mass. (The local fracture zones and the eastern regional zone are confirmed by i.a. increased fracturing in the drill cores).

The regional fracture zones intersect the bedrock and divide it into different blocks. Between these regional fracture zones local fracture zones occur which further divide the bedrock blocks (the rock mass), see Figure 2.1. The rock mass thus comprise rock characterized by "normal" fracturing which can not be traced or followed as zones of distinct extension.

In the site the bedrock is composed of alternating strata of veined gneiss and granite gneiss. The orientation of the strata follows the general north-east strike and vertical dip that characterize the bedrock structure. The granite gneiss constitutes approximately 3 per cent of the rock.

The site Fjällveden is situated on the water divide between two drainage areas. The site is characterized by a flat topography and the altitude varies between 38 and 76 m above sea-level. Based on observations of the groundwater table in the bedrock and the fact that the groundwater table in Sweden, in general, follow the topography, due to the humid climate and low hydraulic conductivity of the bedrock, a groundwater level map has been constructed, see Figure 2.2.

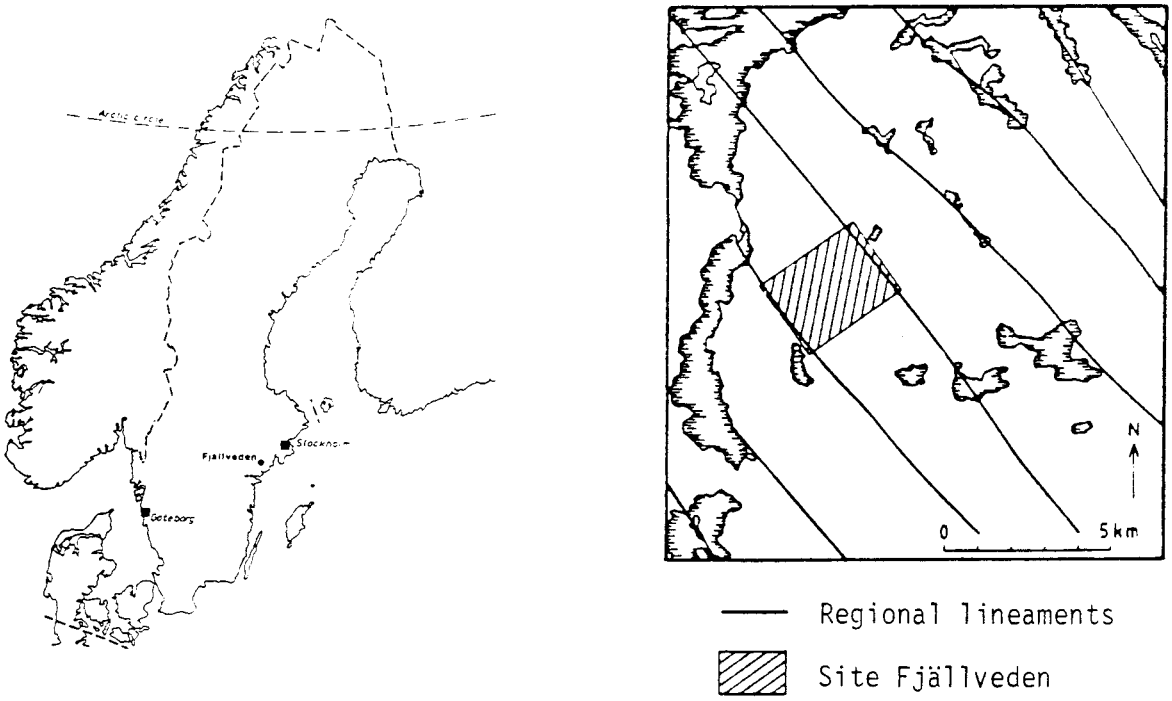

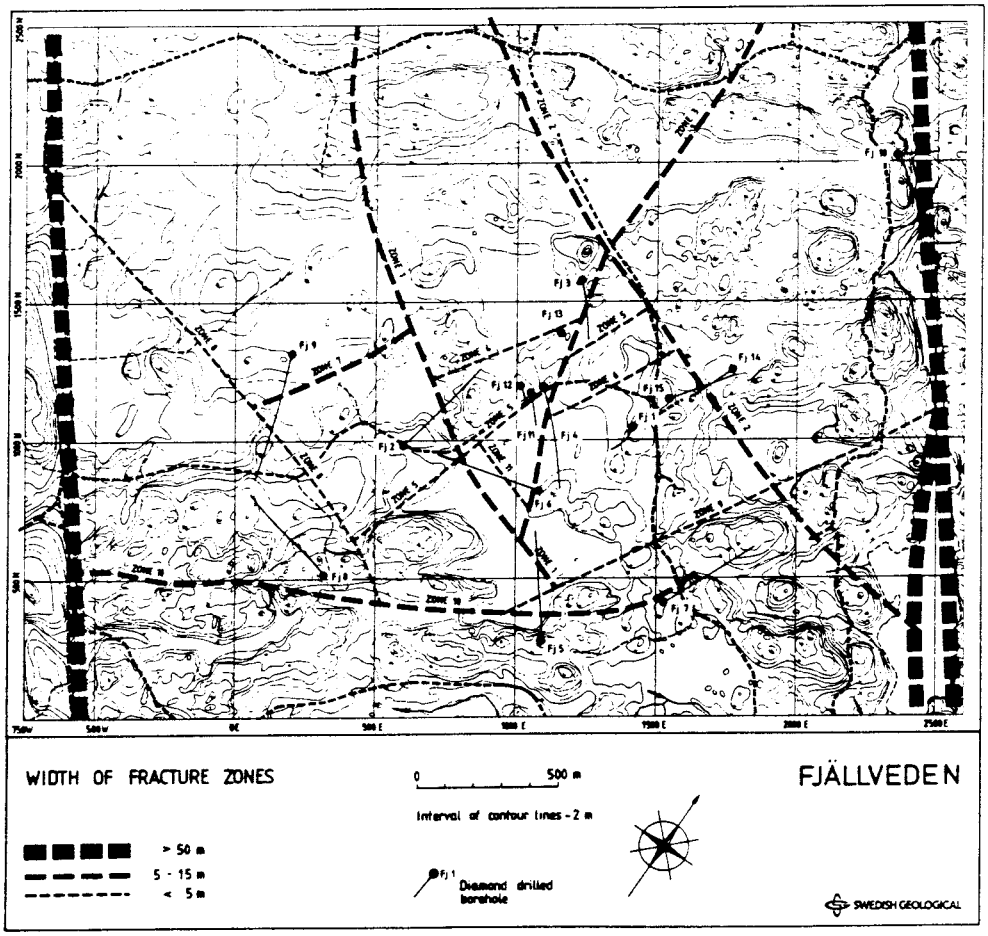

Figure 2.1 The Fjällveden study site, fracture zones and borehole locations.

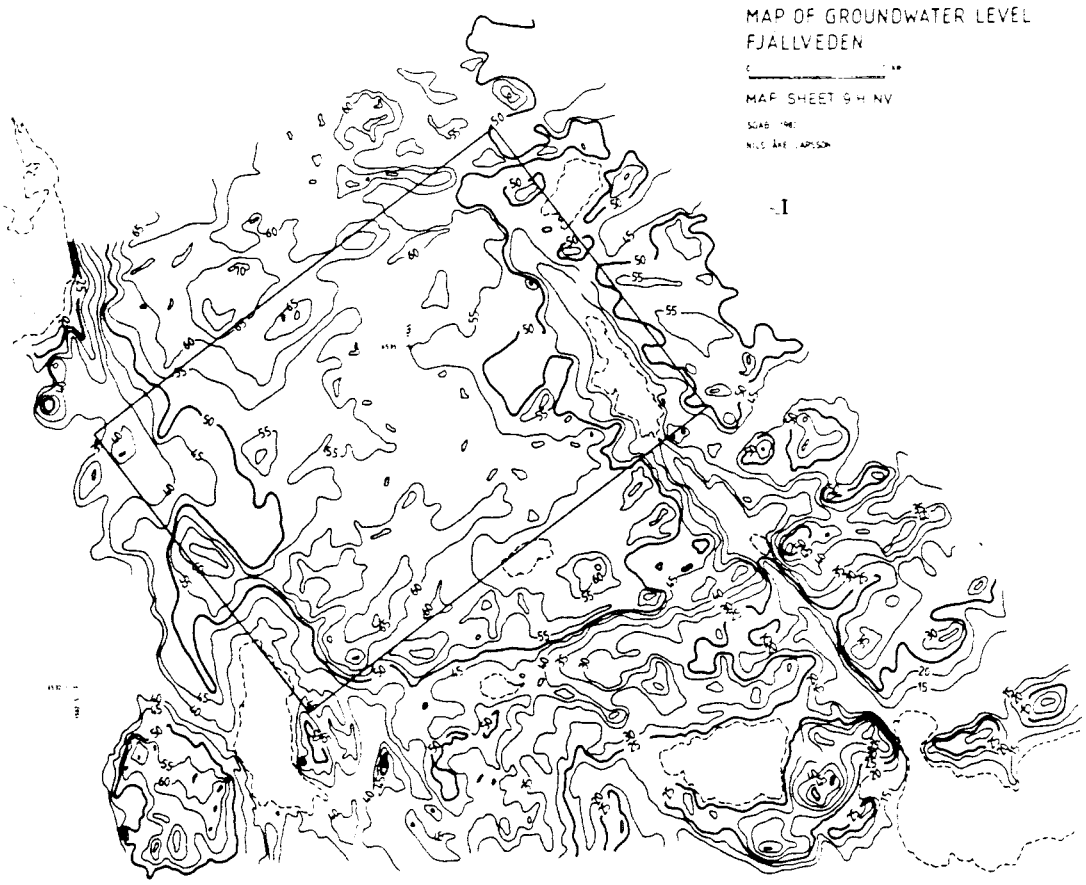

Figure 2.2 Groundwater level map (metre above sea-level) at site Fjällveden.

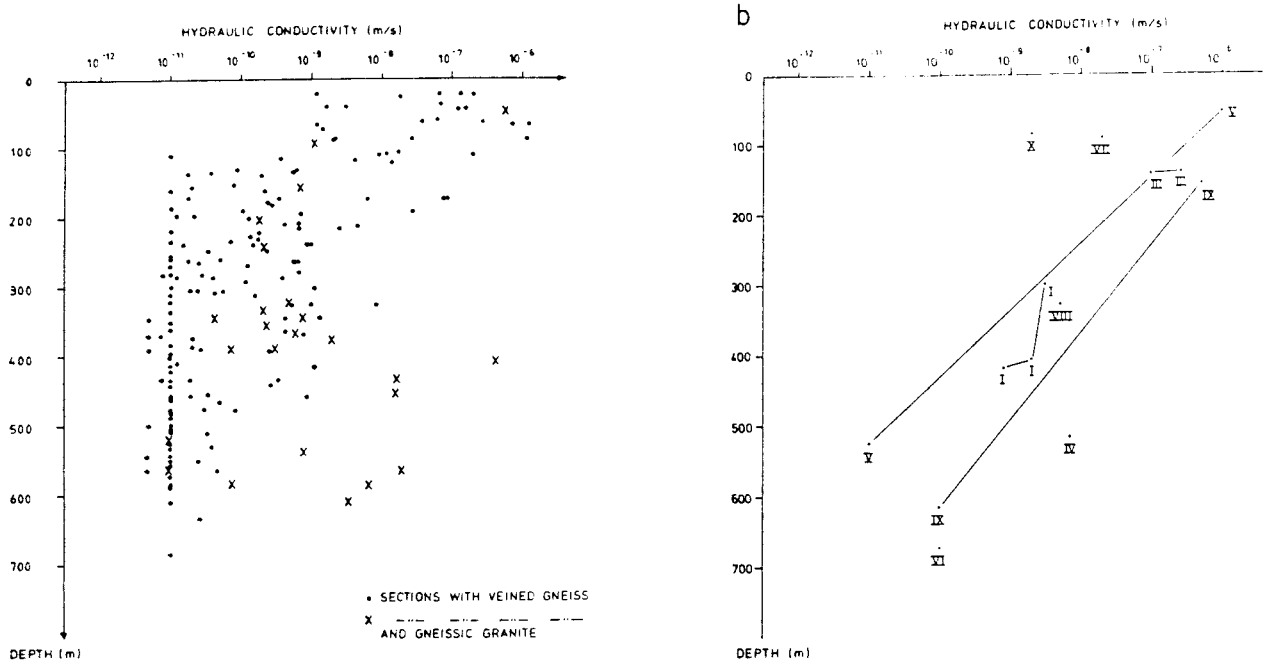

Figure 2.3 Hydraulic conductivity (25 m sections) for the rock mass (a) and local fracture zones (b).

2.2 Hydraulic conductivity of the bedrock

The hydraulic conductivity of the bedrock is dependent on the frequency, apertures and continuity of the hydraulically conductive fractures. The hydraulic conductivity has been determined by water injection tests in 25 m sections in core-drilled boreholes, diameter 56 mm. The sections have been sealed off by means of inflatable rubber packers and a total of 219 tests (i.e. 200 in the rock mass and 19 in the local fracture zones) have been carried out, see Figure 2.3.

Each individual measurement value represents a limited part of the bedrock. The size of these part varies and depends on the hydraulic conductivity and the storativity.

For numerical model calculations of the groundwater head and flow, the hydraulic conductivity has to be given as a constant or as a function in space, referred to as the effective hydraulic conductivity, K_e. This effective hydraulic conductivity constitutes some kind of mean value of all individual conductivities measured (within a hydraulic unit).

The interrelations between these parts are decisive on the choice of mean value estimation, see Figure 2.4. In case (a) each measured K-value represents bedrock strata of infinite extension. With a groundwater flow parallel or perpendicular to the strata, the effective hydraulic conductivity is described by the arithmetic (K_a) and the harmonic (K_h) mean value, respectively.

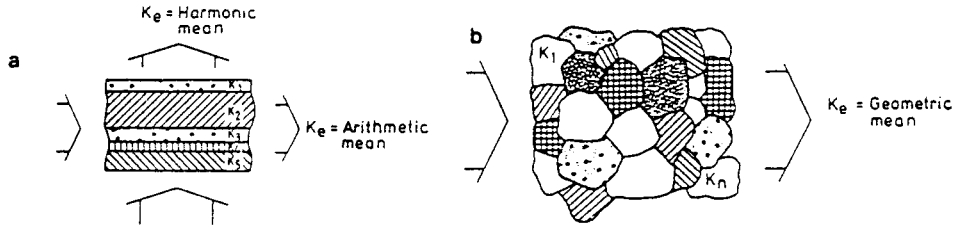

Figure 2.4 Different mean value concepts for the calculation of the effective hydraulic conductivity K_e. The arrows indicate the direction of groundwater flow.

In the different hydraulic units the hydraulic conductivity values are assumed to be of random distribution in space, case (b) in Figure 2.4. Furthermore, the statistical distribution of K-values in each hydraulic unit is assumed to be log-normal, which also has been shown for the rock mass (unit) in Fjällveden by Carlsson et al, 1983.

Dagan (1979 and 1981) has demonstrated that, for a porous statistically homogeneous medium, the effective hydraulic conductivity, K_e, of a log-normal distribution can be expressed as

$$K_e = K_g (1 + (1/2 - 1/m) s^2) \qquad (2\text{-}1)$$

where K_g = the geometric mean value
m = 1, 2 or 3 depending on flow conditions being one-, two- or three-dimensional
s = standard deviation of ln (K)

In a log-normal distribution K_g is equal to the median value. Furthermore, the arithmetic and harmonic mean values can be expressed as

$$K_a = K_g e^{s^2/2}$$

$$K_h = K_g e^{-s^2/2}$$

For a local fracture zone as a whole, the distribution of hydraulic conductivity is assumed to be log-normal. The available data on hydraulic conductivity is, however, too limited to verify this assumption and effective hydraulic conductivity of the local fracture zones is calculated both as geometric and arithmetic mean values. The groundwater flow is assumed to be two-dimensional in the zones.

The alternating strata of veined gneiss and granite gneiss in the site, having different hydraulic conductivities, Figure 2.5, give the rock mass (unit) anisotropic hydraulic properties. In direction parallel or perpendicular to the orientation of the strata, the rock mass has an effective hydraulic conductivity

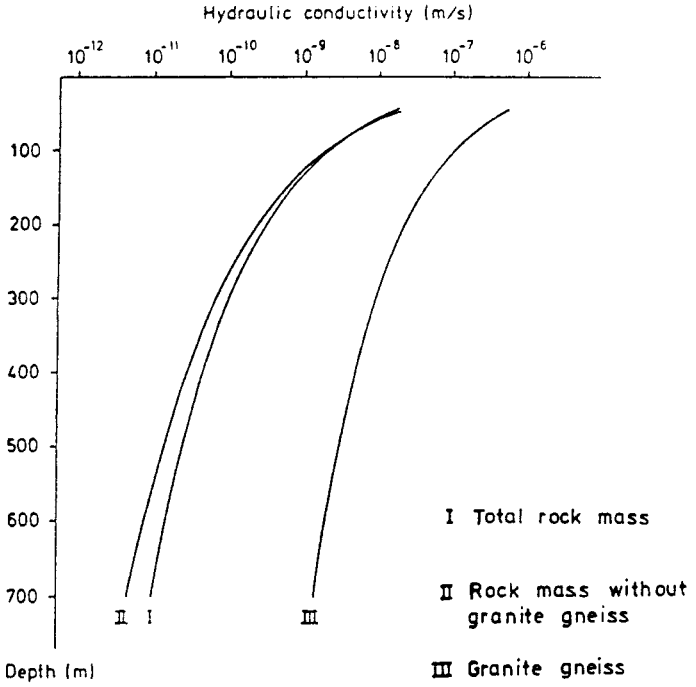

Figure 2.5 Relation between hydraulic conductivity and depth in different rock types within the rock mass.

represented by the arithmetic and harmonic mean of the two rock types respectively (Carlsson et al, 1984).

The aperture of fractures is affected by the rock stress and as the rock stress increases with depth the hydraulic conductivity is expected to decrease. Assuming that the fracture aperture is inversely proportional to the stress, a relationship between depth representing the rock stress and hydraulic conductivity may be expressed as:

$$K = a\, Z^{-b} \qquad (a,b,Z > 0) \qquad (2\text{-}2)$$

where a and b are constants

Z = vertical depth below ground surface

This relationship provides that a change in stress normal to the fracture will result in a reversible change in fracture aperture at any location which is proportional to the original aperture at that location. This is a simplification of a complex process and does not account for the crushing of asperities

or the creation of new points of contact, along the individual fractures (Neuzil and Tracy, 1981).

The depth dependence of the effective hydraulic conductivity may thus be expressed, in accordance with equations (2-1) and (2-2), as:

$$K_e = c\ a\ Z^{-b} = A\ Z^{-b} \qquad (Z > 0) \qquad (2\text{-}3)$$

$$c = (1 + (1/2 - 1/m)\ s^2) \qquad (2\text{-}4)$$

An approximate 98% confidence interval for the regression line is calculated utilizing the Boole-Ferroni inequality for the set of conductivity data for the rock mass. In this context due consideration has been taken to the variance s^2 in equation (2-4). Figure 2.6 shows the calculated regression curve, the confidence interval and the measured data for the study site Fjällveden.

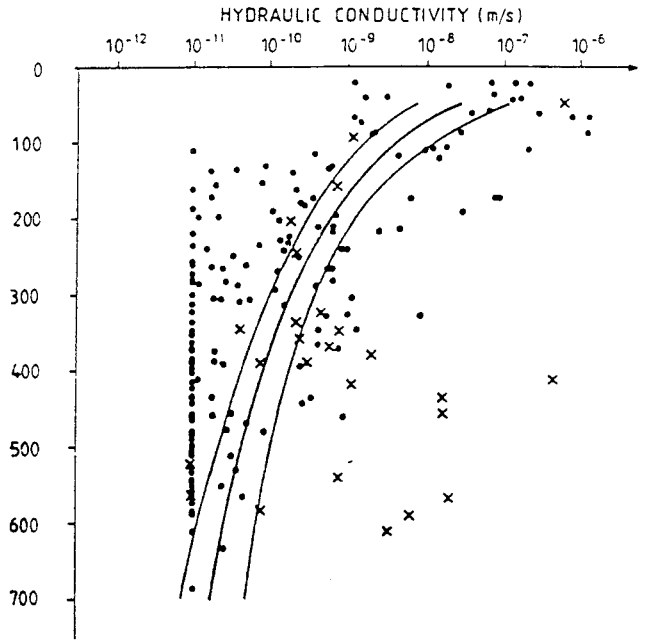

Figure 2.6 Calculated effective hydraulic conductivity versus depth with a confidence interval of 98% for the rock mass at Fjällveden assuming three-dimensional groundwater flow.

Very few data exist on the hydraulic conductivity in the regional fracture zones. Based on data from the Svartboberget study site these zones are assigned a hydraulic conductivity ten times that of the local fracture zones, Ahlbom et al 1983c.

2.3 Physical cases

A total of nine cases with different material properties have been prepared and these are summarized in Table 2.1 and Figure 2.7. Cases 1 to 3 constitute the model runs that were performed during the KBS 3-project, of which aim was to demonstrate that suitable locations for a repository for high-level waste existed (Carlsson et al, 1983). From these, Case 2 is the main alternative as consideration to alternating strata of veined gneiss and granite gneiss with different hydraulic properties has been taken.

Cases 4 to 6 are all variations of Case 2 where different hydraulic conductivity functions for the local fracture zones have been constructed in order to illustrate the influence on the groundwater flow conditions.

Table 2.1 Parameters describing the relationship between effective hydraulic conductivity and depth according to equations (2-3) and (2-4), and number of data, N.

Case	Rock mass					Fracture zones			
	A (m/s)	b	K_e (m/s)	m	N	A (m/s)	b	K_e (m/s)	N
1	$1.5 \cdot 10^{-3}$	2.78	K_g	3D	200	0.17	3.15	K_g	14
2 NE & vert.	$2.8 \cdot 10^{-4}$	2.36	K_a	2D	200	= case 1			
NW	$3.4 \cdot 10^{-3}$	3.11	K_h	2D					
3	= case 1					-	-	-	-
4 0-260 m	= case 2					$3.12 \cdot 10^{-7}$	-	K_a	6
> 260 m						$2.26 \cdot 10^{-9}$	-	K_a	8
5	= case 2					2.29	3.15	K_a	14
6	= case 2					$5.12 \cdot 10^{-9}$	-	K_g	14
7 0-100 m	$6.3 \cdot 10^{-8}$	-	K_g	3D	23				
100-220 m	$1.1 \cdot 10^{-9}$	-	K_g	3D	40	= case 1			
>220m NE&vert.	$2.9 \cdot 10^{-9}$	0.49	K_a	2D	137				
NW	$3.0 \cdot 10^{-5}$	2.32	K_h	2D					
8 zone near	$3.9 \cdot 10^{-2}$	3.13	K_g	3D	27				
NE&vert.	$6.8 \cdot 10^{-4}$	2.53	K_a	2D	173	= case 1			
NW	$1.2 \cdot 10^{-3}$	2.93	K_h	2D					
9 NE&N	= case 8					$4.5 \cdot 10^{-2}$	3.02	K_g	8
NW						7.6	3.73	K_g	4

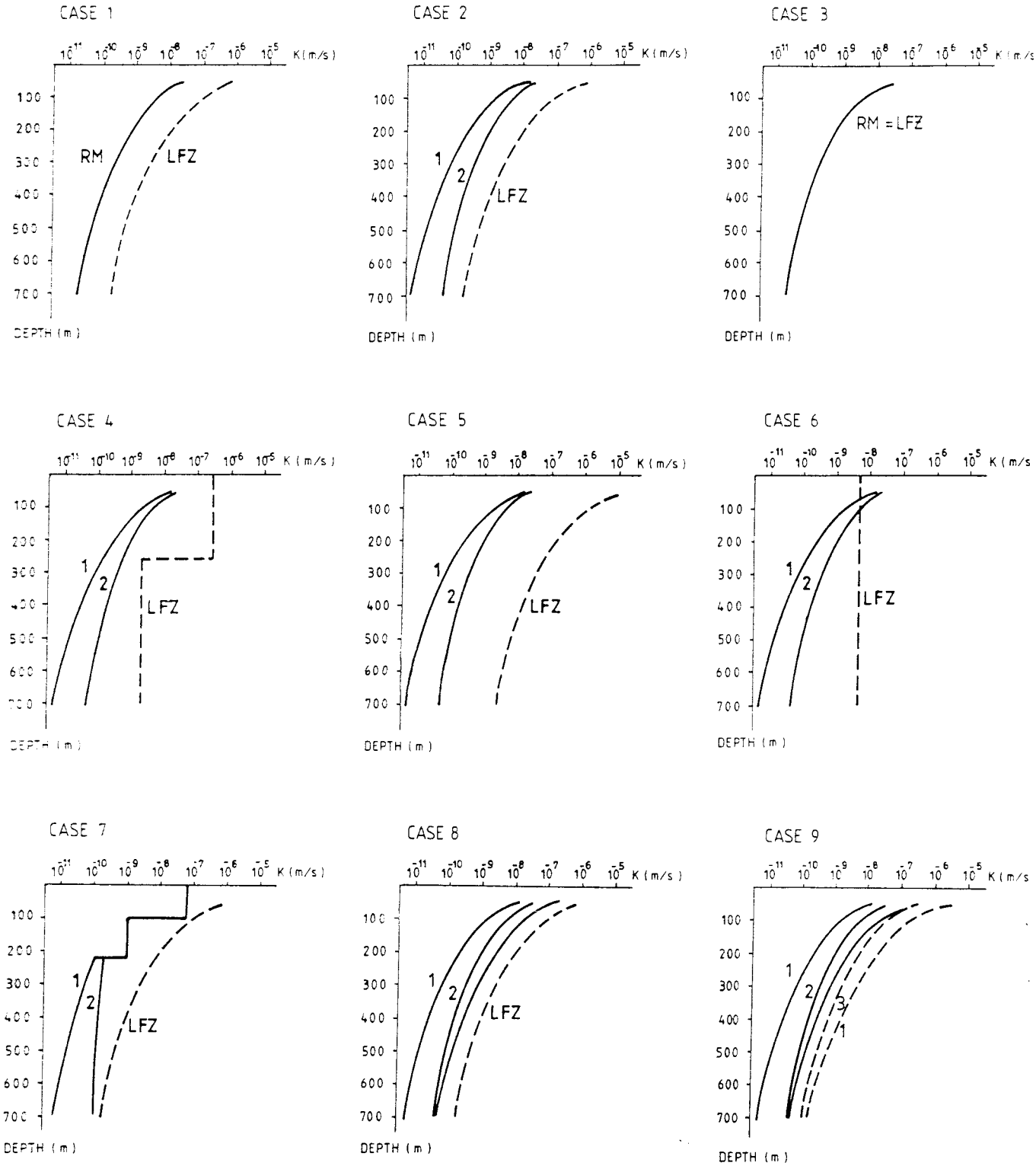

Figure 2.7 Hydraulic conductivity versus depth for rock mass (RM) and local fracture zones (LFZ) for the modelled cases of the Fjällveden study site. 1 = NW direction and 2 = NE & vertical direction and 3 = NE & N direction.

Cases 7 and 8 are again variants of Case 2. In these cases the hydraulic conductivity functions for the rock mass unit has been altered. Finally, Case 9 - an extension of Case 8 - is the only case that has taken into consideration the effect of fracture zone orientation on the hydraulic conductivity.

Case 1

The rock mass has an isotropic hydraulic conductivity. The K(z)-function is based on equation (2-2) and on 200 data points which are assumed to be of random distribution, i.e. $K_e = c\ K_g$. Furthermore, the groundwater flow is regarded as being three-dimensional (m = 3). The regression coefficient was calculated to $r^2 = 0{,}44$.

For the local fracture zones the groundwater flow is considered being two-dimensional and the very few data points (N = 14) as being randomly distributed. The curve fitting $r^2 = 0.58$ is slightly better than for the rock mass.

Case 2

The rock mass is anisotropic due to the alternating strata of the two rock types exhibiting different hydraulic conductivity. In direction parallel, K(NE & vertical), and perpendicular, K(NW), to the orientation of the strata, the rock mass has a hydraulic conductivity represented by the arithmetic and harmonic mean of the two rock types, respectively (cf. Figure 2.4.a):

$$K(\text{NE \& vert.}) = a\,K(GG) + (1-a)\,K(VG) \qquad (2\text{-}5)$$

$$1/K(NW) = a/K(GG) + (1-a)/K(VG) \qquad (2\text{-}6)$$

where K(GG) = the hydraulic conductivity of the granite gneiss
K(VG) = the hydraulic conductivity of the veined gneiss
a = the proportion of granite gneiss (3 per cent)

When estimating the hydraulic conductivity of the veined gneiss, data from sections containing only veined gneiss form the basis for a relationship between depth and effective hydraulic conductivity for this rock type.

In the sections constituted of granite gneiss and veined gneiss the measured conductivity value is reduced with the hydraulic conductivity of the veined gneiss derived from the mentioned relationship. Residual hydraulic conductivity is referred to the granite gneiss as:

$$K(GG) = (K\ L - K(VG)\ L(VG)) \ /\ L(GG) \qquad (2\text{-}7)$$

where L = length of measurement section (25 m)
$L(VG)$ = length of veined gneiss in the measurement section
$L(GG)$ = length of granite gneiss in the measurement section
K = measured hydraulic conductivity
$K(VG)$ = the hydraulic conductivity of veined gneiss at specified depth derived from the depth relation curve

Figure 2.8 shows the effective hydraulic conductivity of veined gneiss and granite gneiss as funcions of depth in the Fjällveden site. The figure also specifies the highest hydraulic conductivity, K (NE & vert.), calculated to illustrate anisotropic conditions.

Moreover, the curve for veined gneiss in fact coincides with the K(z)-function for the perpendicular direction, K(NW). It is also interesting to note that the granite gneiss function exceeds the K(z)-function for the local fracture zones in the present case (= Case 1), except for the uppermost 100 m.

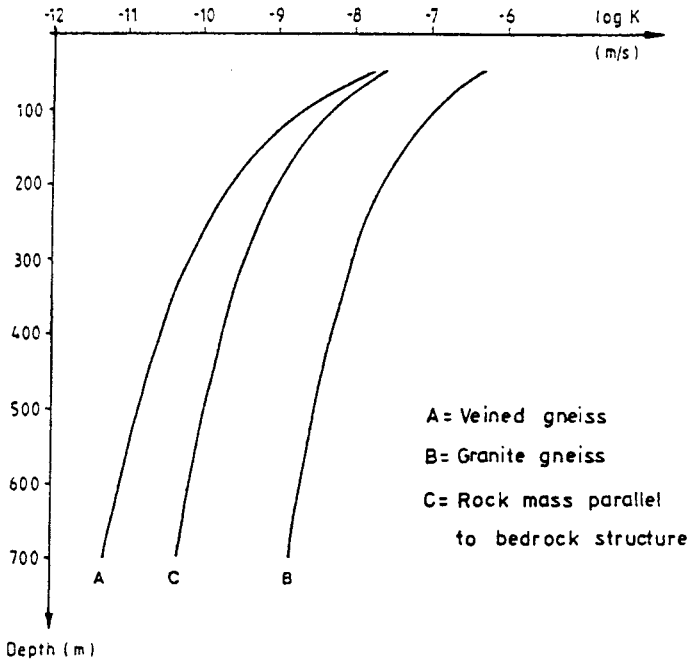

Figure 2.8 Hydraulic conductivity versus depth for veined gneiss, granite gneiss and rock mass parallel to the bedrock structure at Fjällveden.

Case 3

The local fracture zones have been included in the rock mass with isotropic hydraulic properties and the same K(z)-function as in Case 1.

Case 4

The same anisotropic rock mass as in Case 2. The local fracture zones have been assigned a stepwise constant hydraulic conductivity based on arithmetic means above and below 260 m depth. The calculated constants are based on six and eight data points, respectively.

The approximately upper two-hundred metres of the fracture zones usually have a higher hydraulic conductivity assumed to be the result of the glaciation process (Carlsson et al, 1984).

Case 5

The same anisotropic rock mass as in Case 2. For the local fracture zones a depth dependent arithmetic hydraulic conductivity have been calculated, which implies that the fracture zones are hydraulically stratified - a condition without any support from the limited data set. Still, the case represents a "worse case" of Case 2.

Case 6

The same anisotropic rock mass as in Case 2. The local fracture zones have been assigned a constant effective hydraulic conductivity based on the geometric mean i.e. the 14 data points represents a sample of a true random distribution of K-values. This case more illustrates an extreme varity than a realistic one.

Case 7

In this case the rock mass is looked upon as being homogeneous (with respect to the hydraulic properties of the rock types) down to approximately 220 m and heterogeneous under that. The homogeneous part is further divided in two separate blocks at 100 m depth.

The basis for this division is illustrated in Figure 2.3; the higher conductivities of the granite gneiss appears first at greater depth, and the variations in hydraulic conductivity differs significantly for these three parts of the rock mass. In the uppermost 100 m the hydraulic conductivity is greater than 10^{-9} m/s and beneath 220 m only sections including granite gneiss exceed that value. The section 100-220 m depth represents a transition zone with conductivities ranging from 10^{-11} m/s to 10^{-7} m/s.

The effective hydraulic conductivity (K_e) is consistently represented by a stepwise constant geometric mean down to 220 m depth and by anisotropic hydraulic properties, in accordance with Case 2, beneath 220 m depth.

The local fracture zones are identical with Case 1.

Case 8

The basic concept for the actual case is that the rock mass adjacent to the local fracture zones may show diverging hydraulic properties from the rest of the rock mass. This "zone near" rock mass comprises a single set of 25 m test sections surrounding the local fracture zones, making up a total of 27 data points. Each data point represents a bedrock width of approximately 10 to 20 m depending on the inclination of fracture zone and borehole, respectively.

In the "zone near" rock mass the groundwater flow is assumed to be three-dimensional. Depth dependence of the effective hydraulic conductivity is calculated according to equation (2-3). The regression coefficient $r^2 = 0.59$.

Based on the remaining rock mass data (N=173 data points), representing the relatively intact rock, an anisotropic hydraulic conductivity is assigned in accordance with Case 2.

The hydraulic conductivity of the local fracture zones is identical with the conditions in Case 1.

The depth dependence of the hydraulic conductivity is almost the same for the local fracture zones and for the "zone near" rock mass (i.e. b = 3.15 and b = 3.13 respectively). This consistency expires if the width of the "zone near" rock mass is doubled, i.e. two pair of 25 m sections surrounding the fracture zones. In fact, the depth dependence for the "zone near" and the residual rock mass (being treated as isotropic) is then in good agreement.

Case 9

This case is a further development of Case 8, and comprises division of the local fracture zones with respect to the orientation of the zones. The effective hydraulic conductivity of the NE and NW striking local fracture zones are separately calculated in accordance with equation (2-3) and assuming two-dimensional groundwater flow. The N striking fracture zones are given the same K(z)-function as the NE striking.

2.4 Comparison of the cases

The nine cases presented above can be classified with respect to their reliability of describing the geologic-hydrogeological conditions of the Fjällveden study-site.

The most realistic cases are considered to be Case 2 and Case 8. Case 2 has adopted that the rock mass is stratified with rock types of different hydraulic properties and that the hydraulic conductivity of the local fracture zones is randomly distributed (i.e. $K_e = K_g \times c$). In Case 8 the importance of the local fracture zones is accentuated as a "zone near" rock mass with greater hydraulic conductivity is identified. The hydraulic properties for the rest of the rock mass is practically the same as in Case 2.

The Cases 9 and 5 are variants on the two previous cases and illustrate the influence of rock stress on the hydraulic conductivity of the local fracture zones with respect to fracture zone orientation and bedrock load, respectively. Both cases are, however, based on very few data points; e.g. the use of arithmetic means (Case 5) implies stratified layers of different hydraulic conductivity in the fracture zones - an assumption which can not be verified from available data.

The second group of cases is characterized as possible ones. In Cases 7 and 4 the stepwise decrease in hydraulic conductivity and constant arithmetic means in the fracture zones (Case 4)

lack logical explanation, a more continuous change would be more likely.

Case 1 disregards that the rock mass in the Fjällveden site is stratified and anisotropic. Case 1 becomes most realistic only if the extension of the layers of granite gneiss is not continuous.

The last group, Case 3 and 6, comprises "variation cases" that mainly are constructed to illustrate the influence of different extreme conditions.

3. GROUNDWATER FLOW MODEL

3.1. Numerical model

The mathematical model used in this study is a three-dimensional model based on the Finite Element Method. The name of the code is GWHRT (Thunvik and Braester 1980). The code is designed for treating transient and steady-state problems including thermal buoyancy and partially saturated flow. In the current application for the Fjällveden site, steady-state flow with constant fluid properties under saturated conditions have been assumed.

The principal data needed for this simulation are divided into the following groups:

- Geometry description of the site and its different hydraulic units.

- Boundary conditions of the modelled area

- Material properties of the different hydraulic units

In order to facilitate the handling of input and output data from the code a program package called HYPAC has been used (Grundfelt, 1983).

GWHRT is implemented on a Amdahl-470 at Stockholm University Computing Center. All the calculations referred to in this report are computed on this machine.

3.2 Geometry and hydraulic units

A number of model calculations have been performed with various spatial distributions of the hydraulic conductivity.

The area modelled of the Fjällveden site covers approximately 4.1 km^2. The hydraulic units in the modelled domain comprise rock mass, local and regional fracture zones. In some cases a "transition zone" is modelled on the outside of each fracture zone. The width of these zones is equal to the width of the associated fracture zone. The modelled fracture zones in the site area are indicated in Figure 3.1. The modelled fracture zone pattern is somewhat simplified compared to original tectonic map derived from the site investigations, Figure 2.1. Table 3.1 shows a comparison between the widths and dips of the fracture zones as modelled with those obtained from the site investigations. The zones 3 and 5 have been modelled somewhat wider than the measured widths. Zone no 5 has been assigned the transmissivities of zones 4 and 6 that run parallel with zone no 5 and which have been omitted from modelling.

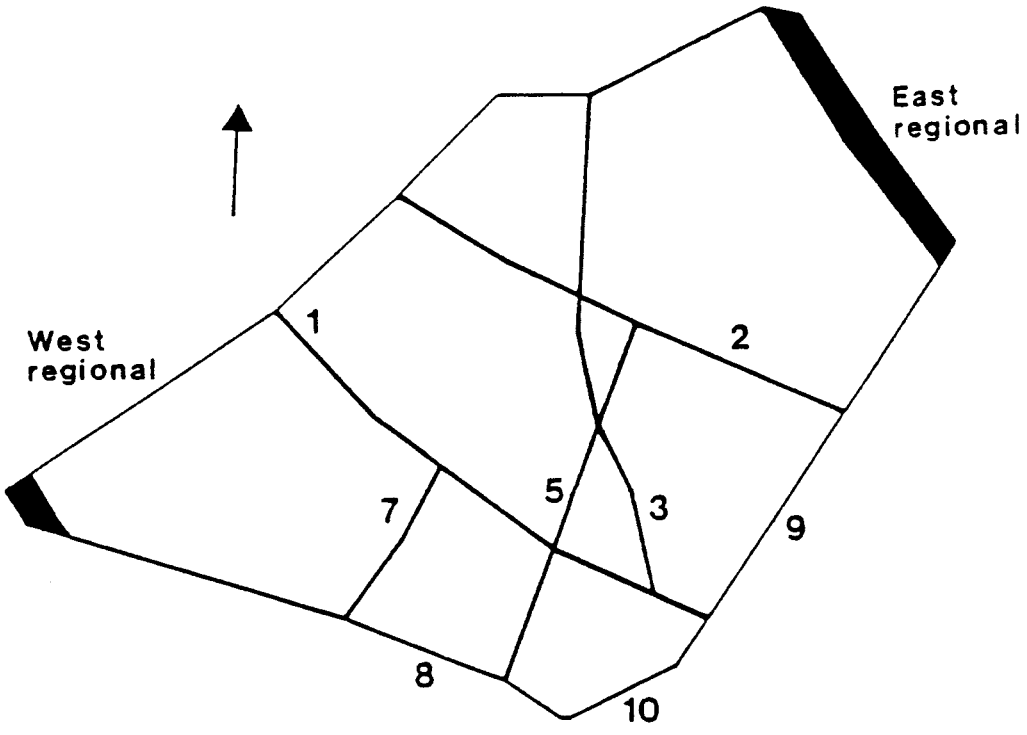

Figure 3.1 Modelled fracture zones at the Fjällveden site.

Table 3.1 Comparison between measured and modelled fracture zones at the Fjällveden site.

Fracture Zone	Measured width (m)	Inclination (degrees)	Modelled width (m)	Inclination (degrees)
1	1-7	90	5	90
2	9-12	80 NE	20	80 NE
3	5-11	90	10	90
4	1	80 SE	-	-
5	0.5-1	80 NW	5	80 NW
6	0.2	75 SE	-	-
7	14	60 NW	14	60 NW
8	4.5	90	5	90
9	5	75 SE	5	75 SE
10	5-6	70 SE	5	70 SE
11	3	90	-	-
Reg	90	75 SE	100	90

The element mesh used consist of 6 horisontal element layers containing a total of 1932 elements. In order to facilitate the description of the groundwater flow in regions where high hydraulic gradients are expected to prevail, the element density is greater in the upper portions of the mesh. The vertical extension of individual elements increases with depth according to a geometric series. The approximate level of the upper surface of each element layer is: 50 m, -100 m, -260 m, -500 m, -830 m and -1170 m. The number of nodal points associated to each cubodial element varies between 8-20 nodes per element. The total number of nodal points is 8538. The element distribution of the top surface is shown in Figure 3.2.

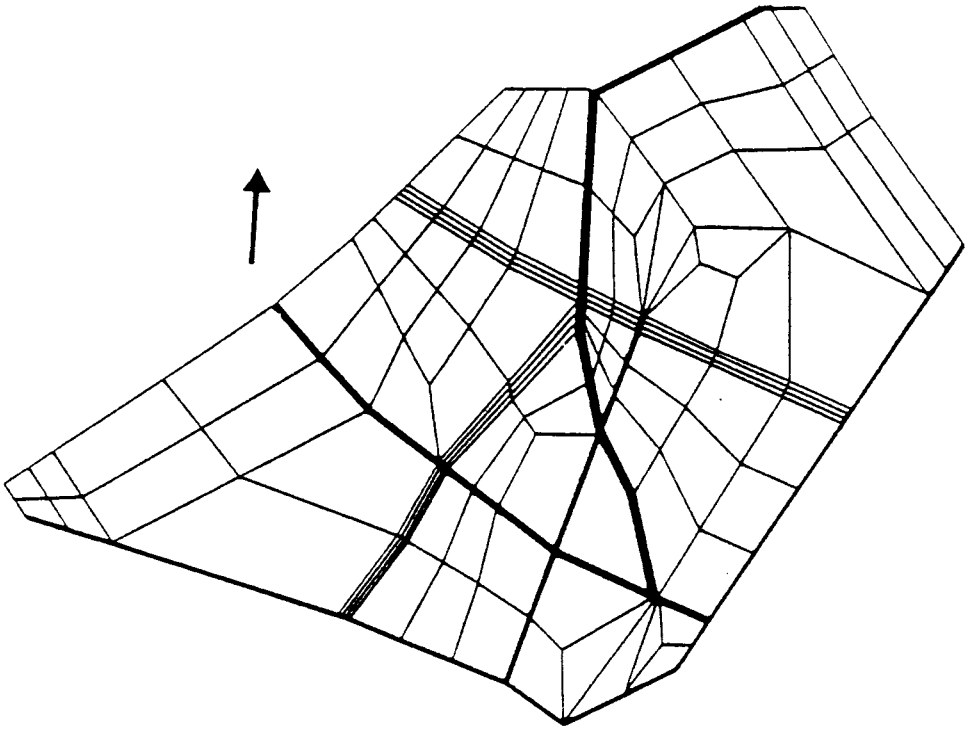

Figure 3.2 Top surface of the element mesh for the Fjällveden site.

3.3 Material properties and boundary conditions

The governing material property of the rock in this study is the hydraulic conductivity. An effective hydraulic conductivity is calculated for each element of the mesh. For the calculation cases in this study the hydraulic conductivity assigned to the elements is assumed either to be constant, or to vary with depth according to a power function, equation (2-3). The value assigned to a given element, a constant, is taken at a depth corresponing to the centeroid of the element. In some cases the hydraulic conductivity is assumed to be anisotropic.

The top surface of the mesh has been adjusted to the level of the groundwater table in the modelled domain. The position of the groundwater table has been arrived at through digitalization of the groundwater map shown in Figure 2.2. The digitized groundwater table is illustrated in Figure 3.3. The pressure assigned to the top surface is set to zero, ie atmospheric pressure. The bottom surface is treated as a non-flow boundary situated 1500m below sea level. All the vertical boundaries except the north-western boundary are defined as non-flow boundaries located at the outer surface of the fracture zones. This means that the flow is forced upwards in these zones. The north-western boundary is a vertical non-flow boundary running along a topographical groundwater divide. Figure 3.4 shows a contour map of the upper surface of the element mesh.

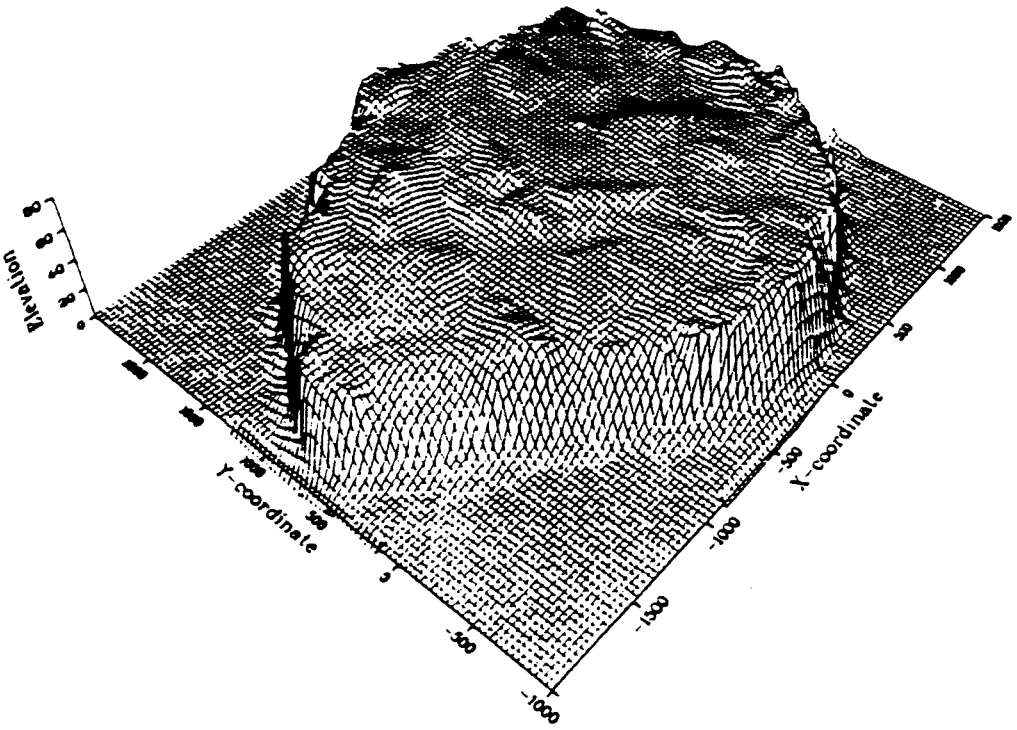

Figure 3.3 Relief map of the groundwater table at the Fjällveden site.

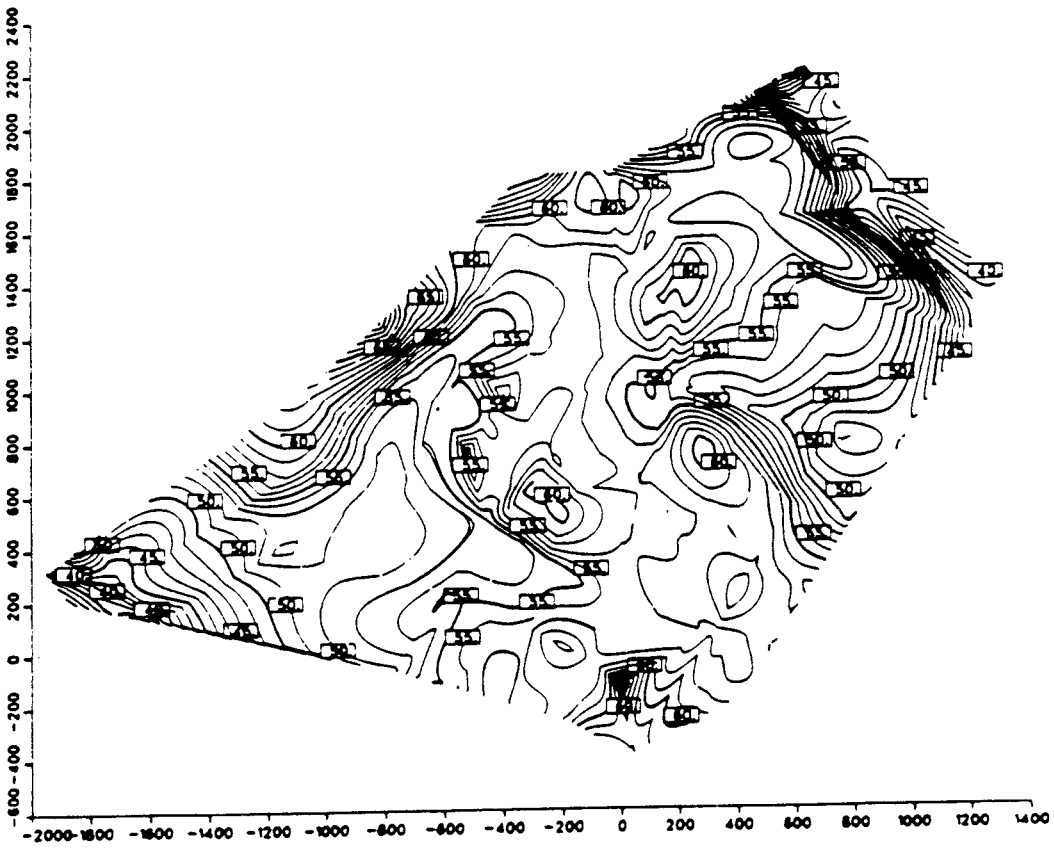

Figure 3.4 Contour map of the groundwater table (metre above sea-level) at the Fjällveden site as it is represented mathematically at the top surface of the element mesh.

4. RESULTS OF THE NUMERICAL MODELLING

4.1 General

The presentation of results is directed towards:

- the distribution of groundwater head and flow field
- the flow rate distribution in the region of the potential repository
- the flux rate at the starting point and particle travel time for a particle released from a given position
- the groundwater recharge rate in the modelled domain
- the mass conservation of the numerical solution for each element

In order to make a comprehensible presentation of the results from this model sensitivity exercise the nine cases have been divided in three main groups as follows:

1. Rock mass variations - Case 1,2,7,8; These cases illustrate the effect of different hydraulic concepts used for the rock mass, see Figure 4.1. In Case 1 the rock mass is treated as an homogeneous medium with isotropic hydraulic properties. On the contrary, the rock mass in Case 2 has anisotropic hydraulic properties as consideration has been payed to that the alternating strata of the two rock types have different hydraulic conductivity.

   Case 7 is, from a conceptual point, a sort of compromise between the previous cases; an isotropic homogeneous rock mass between 0-220 m depth and an anisotropic heterogeneous one at greater depth. The basis for this is the set of test data (e.g. Figure 2.3.a) from which the difference in hydraulic conductivity for the two rock types become evident below approx. 250 m. The homogeneous upper part of the rock mass is further divided into two separate blocks at 100 m depth, each assigned a constant hydraulic conductivity. This stepwise reduction of hydraulic conductivity can be regarded

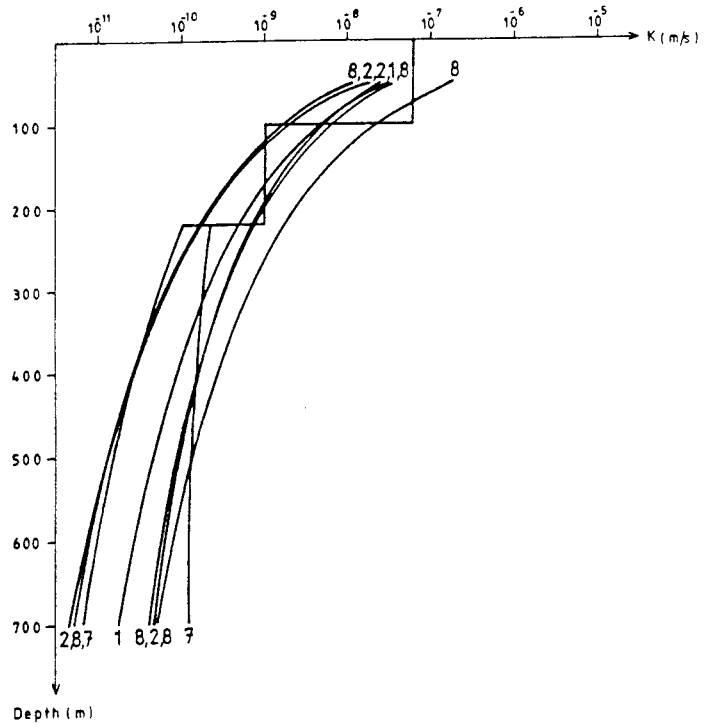

Figure 4.1 Compilation of the K(z)-function for the various rock mass concepts (Case 1, 2, 7 and 8), Fjällveden.

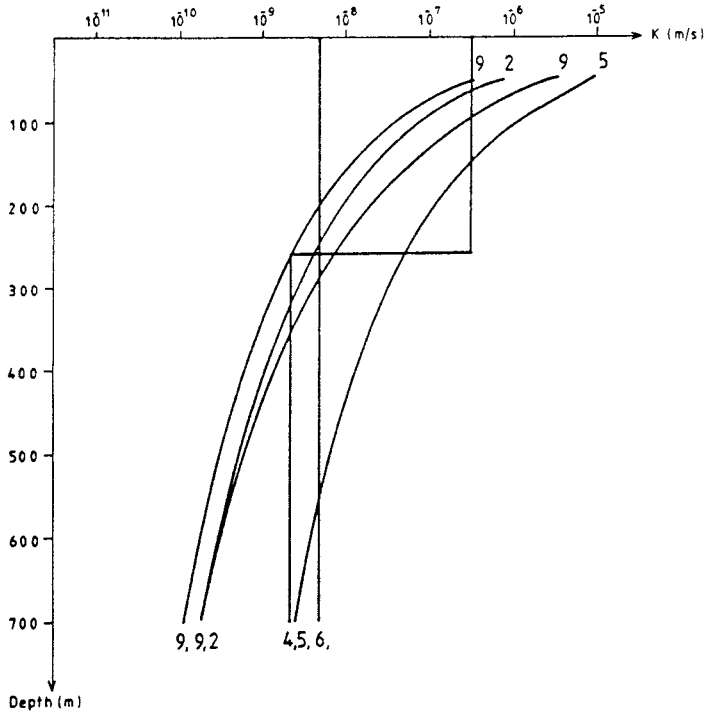

Figure 4.2 Compilation of the K(z)-function for the various concepts of local fracture zones (Case 2, 4, 5, 6, and 9), Fjällveden.

as a "gradually" sealing of the fracture system as the overburden of the bedrock increases with depth.

Finally, Case 8 has adopted the same anisotropic concept as in Case 2, but a "zone near" rock mass is separated from the original data set of the rock mass. As this "zone near" rock mass has greater hydraulic conductivity than the rest of the rock mass the importance of the local fracture zones is increased.

The local fracture zones have identical hydraulic properties for all four cases.

2. Hydraulic contrast between rock mass and fracture zones - Case 1,3; In Case 1 the local fracture zones are assigned a hydraulic conductivity some ten times greater than the rock mass. In Case 3 the fracture zones are given the same hydraulic conductivity as the rock mass and thus no hydraulic contrast exists in this case, see Figure 2.7. This comparison shows the influence of fracture zones with high hydraulic conductivity on the groundwater flow conditions. The two cases have identical rock mass conditions.

3. Fracture zone variations - Case 2,4,5,6,(8),9; The first four cases have identical rock mass and are aimed at demonstrating the effect of using different mean values of the hydraulic conductivity for the fracture zones, see Figure 4.2. The hydraulic conductivity of the fracture zones in Case 2 and Case 5 are depth-dependent and represent two different approaches in calculating the effective hydraulic conductivity (K_e). Case 2 has a hydraulic conductivity based on the geometric mean, which corresponds to a random distribution of K-values. On the other hand Case 5 utilize the arithmetic mean, thus corresponding to a stratified layering of hydraulic conductivities.

In Case 4 and Case 6 the fracture zones are assigned constant arithmetic means, thus using the concept of stratified layering and homogeneous conditions. However, in Case 4 a

stepwise K-function divide the fracture zones in two blocks (at 260 m depth), indicating two different "homogeneous" parts.

As pointed out earlier the limited set of data for the fracture zones does not support any of the concepts used in the report.

Case 9 illustrates the effect of anisotropy for the local fracture zone unit as the fracture zones have been separated in two groups according to their orientation. One group includes fracture zones striking NW and one group zones striking N and NE. The effect of anisotropy is best studied by comparison Case 9 and Case 8 as these have identical rock mass. Furthermore, for Case 9 and 8 a "zone near" rock mass of higher hydraulic conductivity than for the rest of the rock mass is added, which emphasize the role of the fracture zones.

4.2 Groundwater head distribution and flow field

The groundwater head distribution at 500 metre depth (i.e. potential repository depth) for the Cases 1 to 9 are shown in Figure 4.3 and 4.4. The head distribution in vertical cross-sections at four different locations are given in Appendix I.

The general groundwater flow pattern at the 500 m level is characterized by a flow inwards from the the north and the south to a saddle point located in the centre of the modelled domain. From the saddle point the groundwater is drained towards the regional fracture zones in the southwest and the northeast, see Figure 4.3.

The most striking result for the different model cases is the small difference of the calculated groundwater head, both quantitatively and from a distributional point of view. Figure 4.4 illustrates the areal distribution of groundwater head within the model domain. All cases show that 50 % (i.e. mean) of the model domain have a head greater than approx. 54 metre above

sea-level. Furthermore, for Case 3 the groundwater head is greater than 50 m.a.s.l. in 90 % of the domain, while the corresponding head in Case 5 is exceeded in 75 % of the domain. The Figure implies that the hydraulic gradient at 500 m depth is smallest in Case 3 of all cases and consequently greatest in Case 5.

Horisontal isopotential plots of the groundwater head from different depths, not presented here, show that the isopotential curve pattern is dominated by the influence of the groundwater topography down to approximately 500 m depth. Beneath this level the effect of isotropic/anisotropic rock mass can be notified.

- Effect of rock mass variations - Case 1,2,7,8:

The anisotropy skewes the isopotential curves compared to the isotropic Case 1. The isocurves tend to be more directed parallel with the main direction of anisotropy i.e. the horisontal hydraulic head gradient is decreased in the NE-direction and enhanced in the perpendicular NW-direction. This is also evident from the vertical cross-sections 2 and 4, see Appendix I. Vertical 2 is almost NE-directed and the isocurves therefore become more open in Case 2,7 and 8 compared to Case 1. On the contrary, in vertical 4 the isocurves become closer although not as much pronounced as in the previous vertical.

Even in Case 7, where the anisotropy of the rock mass occurs below 220 m this effect is already evident at the 500 m level.

Case 2 and 8 show much the same groundwater flow pattern although the hydraulic gradient in Case 8 is greater probably due to the effect of the "zone near" rock mass with increased hydraulic conductivity.

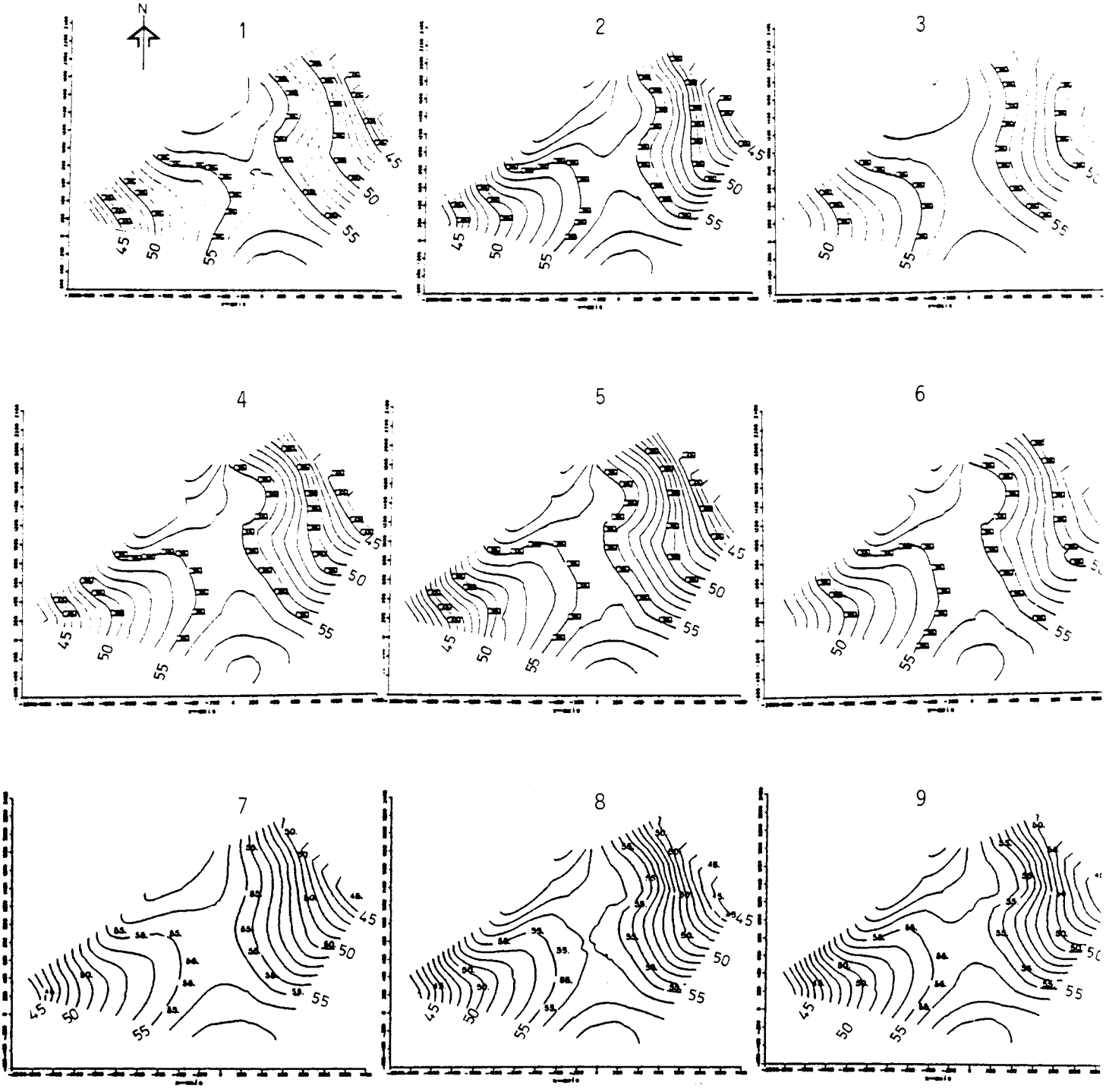

Figure 4.3 Isopotential lines of groundwater head (metre above sea-level) in a horisontal cross-section at 500 m depth for Cases 1 to 9, Fjällveden.

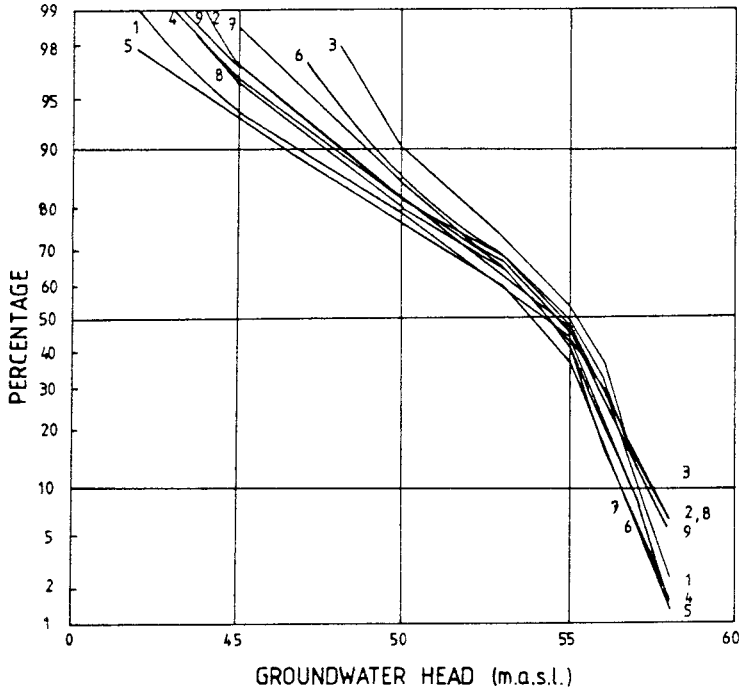

Figure 4.4 Distribution of groundwater head at 500 m depth at the site Fjällveden for Cases 1 to 9, calculated by numerical modelling.

- Effect of hydraulic contrast between rock mass and fracture zones - Case 1,3:

The lack of hydraulic contrast in Case 3 results in relatively small hydraulic gradients and an overall high groundwater head over the modelled domain. Especially the regional fracture zones (with high hydraulic conductivity) at the eastern and the western boundary of the model are responsible for the presence of low hydraulic heads in Case 1, as these fracture zones are situated in the low-lying areas.

- Effect of fracture zone variations - Case 2,4,5,6,(8),9:

The head distribution of Case 2 and 4 is very much the same. For Case 5 and 6, in comparison to Case 2, the hydraulic gradient is increased and decreased, respectively, due to the fact that the groundwater head near the ground surface of highly conductive fracture zones is transfered to great depths. (This partly depends on the properties of the model; the boundary condition of the top surface, the groundwater table, is a constant i.e. the hydraulic gradient at the ground surface does not change with altered K-values. Instead, the groundwater recharge is changed to keep a constant groundwater table). In Case 6 relatively low hydraulic conductivity of the uppermost part of the fracture zones is enough to prevent low hydraulic heads at the 500 m level (cf. Case 4).

The anisotropy in Case 9 does not seem to have any effect on the flow pattern compared to Case 2. However, the effect of hydraulic anisotropy of fracture zones is best studied by comparing Case 9 and Case 8 as these cases have identical rock mass properties. Anisotropic hydraulic conditions for the fracture zones have the same general effect on the hydraulic gradients in the model domain as the introduction of an anisotropic rock mass. Namely, decreased gradients in the NE-direction and increased gradients in the NW-direction. The main direction of anisotropy for the fracture zones is, however, NW-striking and thus not parallel with the direction of decreasing gradient as was the case for the anisotropic rock mass.

The fracture zones constitute a discrete network of highly conductive elements in the model and the changed hydraulic conditions in these (from Case 8 to Case 9) also displace the hydraulic gradients between rock mass and fracture zones. The resulting isopotential pattern is a combination of the interrelated orientation of the fracture zones and their orientation in relation to the isopotentials.

A tendency to changed hydraulic gradients, perhaps caused by the anisotropy of the fracture zones, is the increase and decrease for fracture zones 8 and 9, respectively. A fracture

zone assigned a greater K-value (e.g. zone 8 when changing from case 8 to Case 9) maintain both its low and great groundwater heads to the depth and thus the hydraulic gradient increases at depth. For fracture zone 9 the decreased K-value diminishes the gradient. For the other fracture zones this effect can not be identified, maybe because that this effect is superimposed on other effects within the model domain as distinguished from zones at the boundaries.

Summing up, anisotropic hydraulic properties in the modelled domain, when present in the rock mass, affect the groundwater flow pattern and the isopotential curves are skewed to be parallel to the main direction of anisotropy. In the case of fracture zone anisotropy the isopotentials are skewed to be perpendicular to the main direction of anisotropy. But this effect may vary with the configuration of the fracture zone network. A tendency to effected hydraulic gradients in the fracture zones is visible; the hydraulic gradient is enhanced parallel to the main direction of anisotropy and decreased in the perpendicular direction. The important effect of highly permeable fracture zones is mainly their contribution to maintain high hydraulic gradients at greater depths - a circumstance which is further emphasized by the comparison of Case 1 versus 3 and Case 4 versus 6, respectively.

4.3 Groundwater flow rates

The calculated groundwater flow has been recorded at three levels corresponding to 400 m, 500 m and 600 m depth. Two examples, Case 1 and 2 for the 500 m level, are illustrated in Figure 4.5.

In Figure 4.6 the distribution of the groundwater flow rates over the potential repository area (cf. Fig. 4.5) for the different cases are presented. The calculation results are summarized in Table 4.1 in terms of range and approximate representative values.

Table 4.1 Groundwater flow rate, range and representative value (500 m level) for Case 1 to 9, Fjällveden.

Case	Groundwater flow rate (ml/m^2 year)		
	400 m	500 m	600 m
1	5-25	3-10 (9)	3-10
2	5-50	3-15 (11)	2-15
3	3-25	3-10 (6)	2-4
4	7-50	7-50 (24)	3-15
5	7-50	7-50 (24)	3-15
6	5-50	7-30 (21)	3-15
7	7-50	7-30 (23)	5-30
8	5-50	5-50 (22)	3-15
9	5-50	5-50 (22)	3-15

- Effect of rock mass variations - Case 1,2,7,8:

According to the representative values in Table 4.1 the anisotropic Cases (2, 7 and 8) all show greater groundwater flow rates than the isotropic case, which is a consequence of the general hydraulic gradient in the site being parallel with the main direction of the anisotropy.

The introduction of the "zone near" rock mass with exaggerated hydraulic conductivity (Case 8) increases the flow rate with 100 per cent compared to Case 2 even though the zone near rock mass is a small portion of the total rock mass.

Case 7 and 8 have almost the same average flow rates and the smaller range in Case 7 indicate a more homogeneous flow rate distribution.

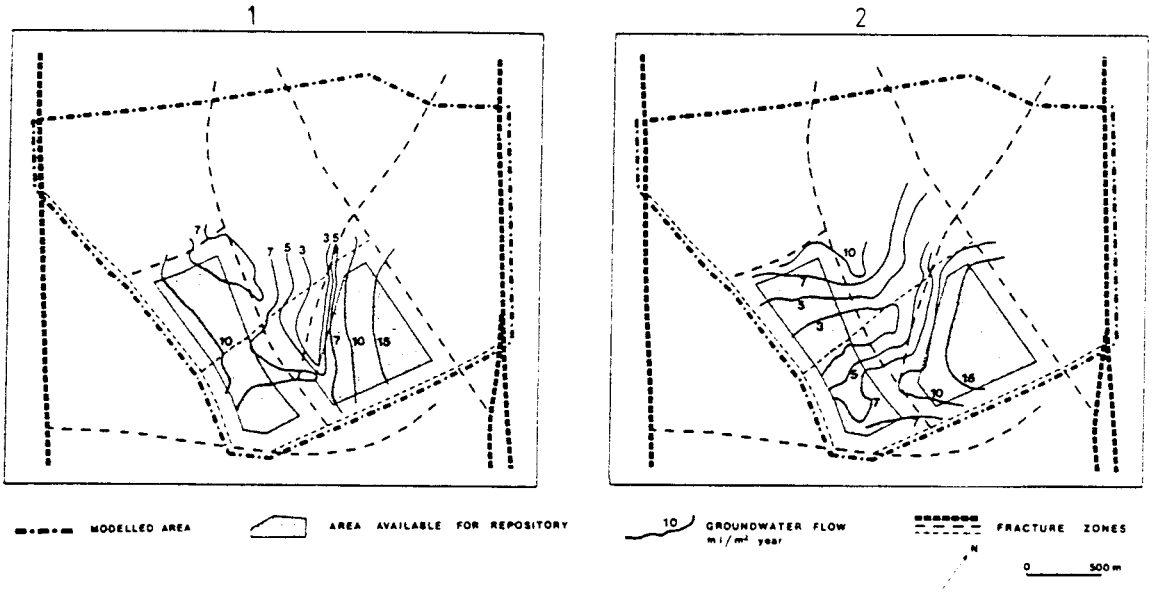

Figure 4.5 Calculated groundwater flow rate distribution (ml/m^2 year) at 500 m depth at the site Fjällveden for Case 1 and Case 2.

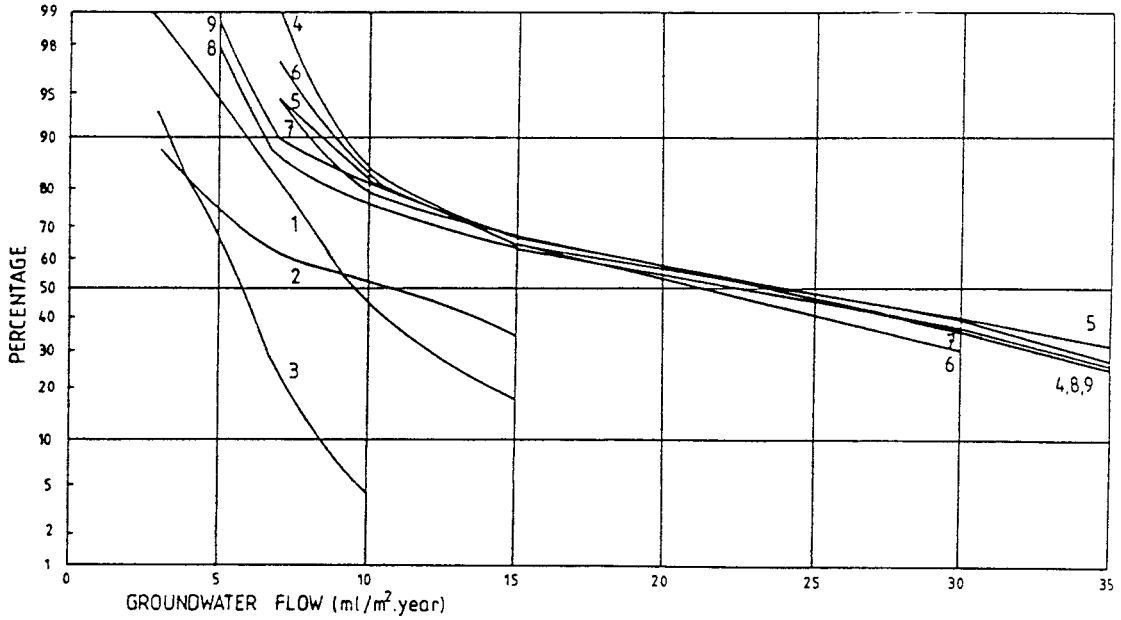

Figure 4.6 Distribution of groundwater flow rate at 500 m depth at the site Fjällveden for Cases 1 to 9, calculated by numerical modelling.

- Effect of hydraulic contrast between rock mass and fracture zones - Case 1,3:

The lack of hydraulic contrast between rock mass and fracture zones causing small hydraulic gradients in Case 3 give consequently rise to low groundwater flow rates.

- Effect of fracture zone variations - Case 2,4,5,6,(8),9:

All cases results in much greater flow rates than the main Case 2 and the difference between these are small on an average basis. The greatest average flow rate is created in the Case 5 and 4, for which the effective hydraulic conductivity is based on arithmetic mean values.

Furthermore, the effect of anisotropy (Case 8 versus Case 9) is insignificant for the Fjällveden site. However, the "zone near" rock mass looked upon as being a widening of the fracture zones have almost the same effect on the flow rates as the arithmetic mean values in Case 4 and 5. A fact that is even more emphasized as the hydraulic conductivity in the "zone near" rock mass (see Case 8, Figure 4.1) is lower than for the fracture zones in the actual cases.

Case 6 having smaller hydraulic gradients at 500 m level than the other cases, show that the hydraulic conductivity is the most important factor in determining the groundwater flow rate.

In summary, the anisotropy of the rock mass increases the groundwater flow rate but to a smaller amount than e.g. the establishment of a "zone near" rock mass with exaggerated hydraulic conductivity.

Highly permeable fracture zones lead to greater groundwater flow rates while the effect of anisotropy for the fracture zones seems to have no influence on the flow rate.

All cases with fracture zone variations give rise to greater flow rates than the main Case 2. The average flow rate for

these cases is much the same but the flow rate range is wider in cases with greater hydraulic contrast between fracture zones and rock mass.

4.4 Particle trajectories

The calculation of particle trajectories in the Fjällveden study comprises the flow rate at a given point (x=365m, y=160m, z=500m) and the particle travel time for a particle released at the same point. The flow lines for the 9 calculation cases are presented in three-dimensional views in Figure 4.8. Starting position and ending positions for the trajectory path ways is illustrated in Figure 4.7. The results are compiled in Table 4.2 below. When calculating the particle travel time the kinematic porosity is assumed to be 1.0 (a fictive value corresponding to the Darcy velocity).

Table 4.2 Flow rate in the particle starting points, ending z-coordinate, path length, particle travel time and average velocity for the flow lines in Case 1-Case 9, the Fjällveden study site.

Case	flow rate	ending	path	travel time	
		z-coord.	length		aver. vel.
	(ml/m^2,yr)	(m)	(m)	(yrs)	(m/yr)
1	4	-476	1070	$1.3\ 10^{8}$	$8.23\ 10^{-6}$
2	11	-478	1075	$6.6\ 10^{7}$	$1.63\ 10^{-5}$
3	3	-136	1490	$1.2\ 10^{8}$	$1.24\ 10^{-5}$
4	10	-295	1345	$7.4\ 10^{7}$	$1.82\ 10^{-5}$
5	11	-357	1625	$6.6\ 10^{7}$	$2.46\ 10^{-5}$
6	10	28	1615	$7.3\ 10^{7}$	$2.21\ 10^{-5}$
7	23	-282	1520	$4.8\ 10^{7}$	$3.17\ 10^{-5}$
8	10	-315	1500	$7.8\ 10^{7}$	$1.92\ 10^{-5}$
9	10	-100	1715	$7.5\ 10^{7}$	$2.29\ 10^{-5}$

All path lines are led towards the eastern boundary. They exit the model in the area where the eastern regional fracture zone intersects fracture zone 9.

- Effect of rock mass variations - Case 1,2,7,8:

The anisotropy in Case 2 seems to have small effect on the direction of the path way compared to Case 1. The particle travel time is, however, decreased with a factor 2 because of a higher K-values in the flow direction for the anisotropic case.

The highest flow rates at the starting point is reached for Case 7. The flow line in Case 7 is similar to Case 8 but the flow in the former case is accentuated to be more vertical. This is probably due to the fact that the decrease in hydraulic conductivity with depth is slower in Case 7 i.e. the hydraulic gradients is maintained at greater depths.

The drainage effect of foremost the eastern regional zone is increased when implementing the "zone near" rock mass in Case 8 (cf. Case 2). This leads to a more northernly directed path way for the trajectory in this case, and as for Case 7, the path lengths are essentially longer.

- Effect of hydraulic contrast between rock mass and fracture zones - Case 1,3:

The drainage effect at the boundaries of the model is reduced when the fracture zones are omitted. Under this presumption the trajectory in Case 3 makes a longer trip before exiting the model.

- Effect of fracture zone variations - Case 2,4,6,(8),9:

The comparably low hydraulic conductivity assigned to the shallow portions of the fracture zones in Case 6 prevents the distribution of high potential differences at depth from the ground

surface. This means that the horisontal gradient is repressed and that the vertical flow will be more pronounced compared with the main case (Case 2).

In Case 5 the opposite presumptions prevails; the horisontal gradients are predominant, which makes the trajectory to form a flat path. Case 4 can be regarded as an intermediate case between Case 5 and Case 6.

The anisotropic conditions in the fracture zones (Case 8 versus Case 9) decreases the drainage effect of zone 9 which consequently gives the trajectory a more northernbound path route.

Summing up, the effect of anisotropy in the rock mass and for the fracture zones, respectively, is small but significant when studying the direction of the path ways. The particle trajectories are skewed and given more northernly bounded routes.

The vertical extension of the flow path is dependent on the interrelations between horisontal and vertical hydraulic gradients, and the distribution of hydraulic conductivity.

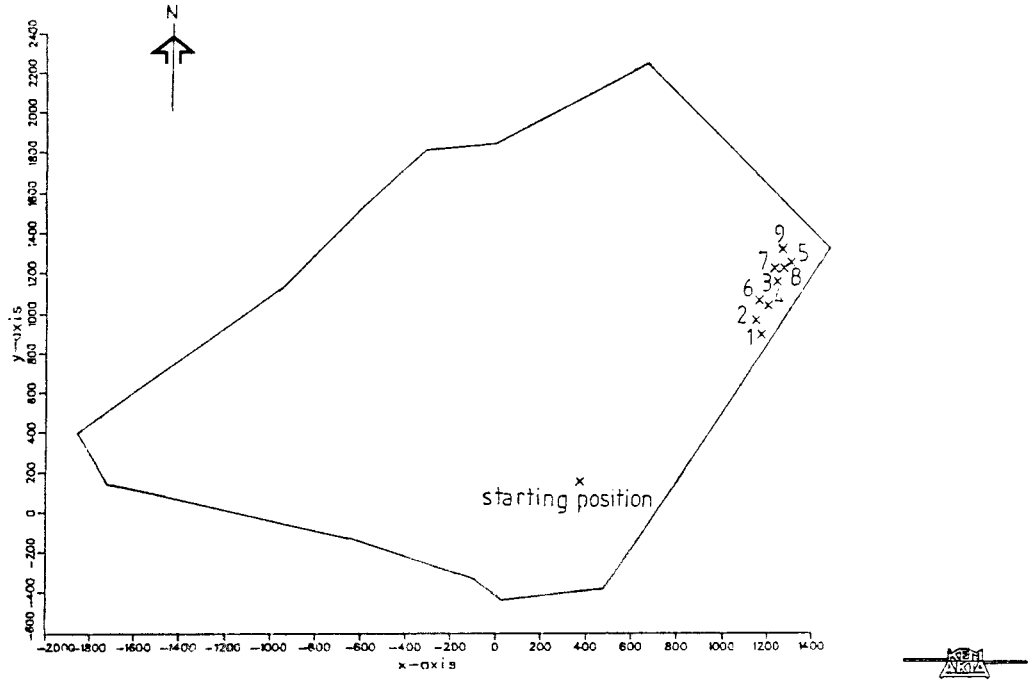

Figure 4.7 Horisontal view showing starting and ending positions of the flow lines in Case 1 to 9.

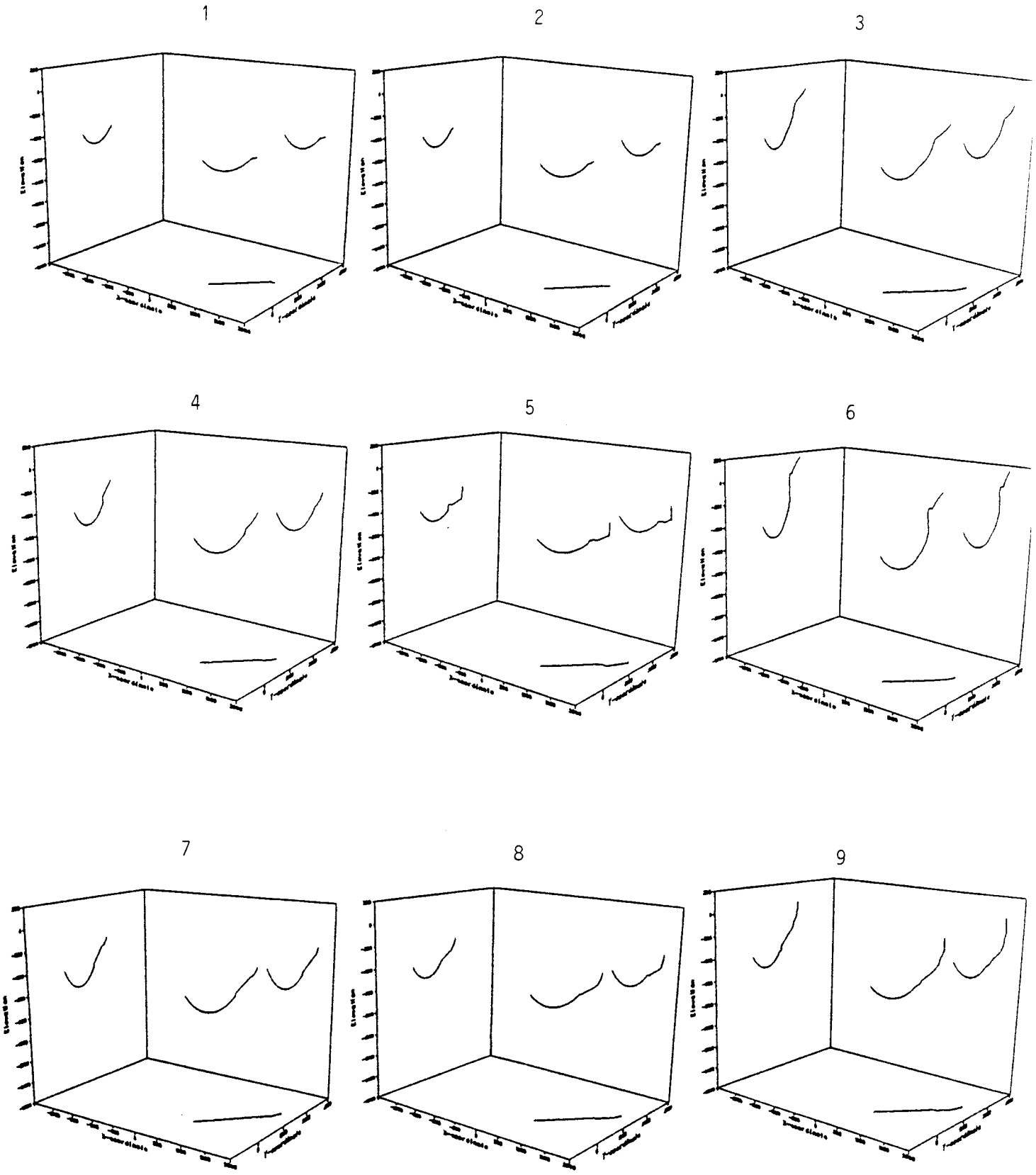

Figure 4.8 Perspective view showing path lines for Case 1-9

4.5 Relevance of results

The relevance of the numerical model calculations is made by means of groundwater recharge and mass balance calculations for the individual finite elements.

4.5.1 Groundwater recharge

The groundwater recharge is calculated as the total recharge across the top surface divided by the area of the top surface of the modelled domain (4.12 km^2). The recharge is also calculated for each hydraulic units separately. The rock mass and the fracture zones constitute 3.91 km^2 and 0.21 km^2, respectively. The resulting groundwater recharge rates are presented in Table 4.2.

Table 4.2 Calculated groundwater recharge and recharge areas for the total area and for the hydraulic units, rock mass (RM) and fracture zones (FZ), separately for Cases 1 to 9, Fjällveden.

Case	Recharge rate (mm/year)				Recharge area (% of total area of hydraul. unit)	
	Total	RM	FZ	FZ/Total	RM	FZ
1	27.9	2.8	25.1	(90%)	70	57
2	-	4.3	-	-	70	-
3	-	1.8	-	-	57	-
4	6.1	2.4	3.7	(61%)	70	48
5	39.1	2.7	36.4	(93%)	68	52
6	1.7	1.8	- 0.1	(0%)	57	19
7	15.7	14.7	1.0	(6%)	53	24
8	5.1	3.6	1.5	(29%)	62	33
9	6.4	3.8	2.6	(41%)	64	38

The calculated recharge rates for the different cases is within the interval expected from the current understanding of the groundwater recharge in crystalline bedrock.

- Effect of rock mass variations - Case 1,2,7,8:

The anisotropy of the hydraulic conductivity causes enlargement of the recharge rate to the rock mass and reduction for the modelled domain as a whole along with that the recharge area of the fracture zones decreases drastically.

For example, in Case 8 the total recharge is reduced by 5 times and the recharge portion of the fracture zones is decreased from 90% to 29% of the total recharge compared to the isotropic Case 1. For Case 7 the latter is further emphasized as the conductivity contrast between rock mass and fracture zones is reduced.

- Effect of hydraulic contrast between rock mass and fracture zones - Case 1, 3:

The lack of fracture zones consequently results in small groundwater recharge rates and a minor reduction of recharge area.

- Effect of fracture zone variations - Case 2,4,5,6,(8),9:

The characteristic of the actual cases is that the recharge ranges are small with two exceptions, namely Cases 5 and 6. These two extremes illustrate the effect of fracture zone conductivity; the former results in the highest recharge rate of all cases while the latter consequently gives recharge rate comparable with Case 3.

Although, the disparity in groundwater recharge between Case 5 and 6 the average groundwater flow rates at potential repository level is much the same (cf. chapter 4.2).

Summing up, variations of hydraulic conductivity in the bedrock, whether these are imposed on the rock mass unit or the fracture zone unit, lead, in principal, to the same results; small recharge change for the rock mass and great disparities for the fracture zones. The corresponding variations are also reflected in the size of the recharge area of the fracture zones.

Finally, for the cases, which in the upper part of the bedrock have the greatest hydraulic contrast between rock mass and fracture zones, the fracture zones have a dominating influence on the groundwater recharge, e.g. Case 1, 5 and 4. For Case 6 and 7 the opposite conditions are valid.

4.5.2 Mass conservation of numerical solution

A mass balance is calculated for each element in the mesh to check the numerical quality of the solution. A relative mass balance deviation is calculated from the following equation.

$$\Delta_e = \frac{\sum_i F_i}{\sum_i |F_i|} \qquad (4\text{-}1)$$

where Δe = relative mass deviation for element e

F = flow through surface i in element e

An element with an completely conservative solution will have a deviation index, e, equal to 0 % with this notation , whereas a deviation index of 100 % will correspond to a flow either only into or out of the element. The portion of the elements in different deviation intervals are given in Table 4.3

Table 4.3 Mass balance for calculation Cases 1to 9, Fjällveden

Case no	Proportion (%) of elements deviating from mass conservation by		
	<1%	1-10%	10-100%
1	22	51	27
2	22	50	28
3	33	44	23
4	22	51	27
5	17	44	39
6	16	46	38
7	22	50	28
8	18	52	30
9	17	54	29

By comparing the figures in Table 4.3 the following can be concluded;

- Effect of rock mass variations - Case 1,2,7,8:

The anisotropy does not seem to affect the numerical solution of the model (Case 1 versus Case 2). In fact, Case 1,2 and 7 have almost identical quality of the solutions. When introducing the "zone near" rock mass in Case 8 the mass conservation is slightly decreased.

- Effect of hydraulic contrast between rock mass and fracture zones - Case 1,3:

The best mass conservation is reached for Case 3, where the fracture zones are omitted, i.e. the hydraulic conductivity contrast is very low.

- Effect of fracture zone variations - Case 2,4,5,6,(8),9:

The relatively bad mass conservation in Case 5 may be caused by high conductivity contrasts in the area of the surficial rock in combination with high hydraulic gradients. The same mass conservation as in Case 5 is reached for Case 6 but here the conductivity contrast is great only at depth and the gradients are everywhere relatively small.

To give a more detailed analysis to the calculation results a thorough check of the mass conservation of each individual element correlated to its location in the element mesh has to be made.

Summing up, anisotropic hydraulic properties of the rock mass, is insignificant to the mass conservation of the numerical solution.

High hydraulic contrasts, especially in areas where high hydraulic gradients prevail, decrease the quality of the solution.

5. DISCUSSION AND CONCLUSIONS

This report has compiled the results from numerical modelling of the Fjällveden study site carried out between the years 1983 - 1987. A total of nine physical cases have been prepared, all based on the same geoscientific data base.

As the numerical model is limited by the amount of geological and hydrological information that can be processed, due to restricted computer work space, the hydrogeological properties of the study site has been simplified. For example, the bedrock is simplified into rock mass, regional fracture zones and local fracture zones. At the preparation of the physical cases these geological features have been considered as individual hydraulic units and assigned different hydraulic properties.

In assigning the nine cases different hydraulic properties the hydraulic conductivity of the rock mass and the local fracture zones has been statistically treated in various ways. The statistical calculations have considered different kind of specific aspects of the geological conditions at the site such as the rock mass being stratified with rock types of different hydraulic conductivity (anisotropy), the increasing rock stress versus depth or the influence of the fracture zones on the adjacent rock mass.

5.1 Summary of results

5.1.1 Comparison of the Cases

The numerical modelling of the cases has given results for the calculated parameters which for each parameter separate the different cases as expected. However, the combined effect of the various parameters, illustrated by the particle trajectories, may for a certain case come out in an unforeseen way.

Furthermore, the basis for some of the cases is, with the present knowledge on the hydrogeological conditions of the Fjällveden site, of equal validity. The numerical modelling has, however, arrived at significantly diverging results.

For example, Case 2 and Case 8, which have been considered as the most realistic cases, show average groundwater flow rates at the potential repository depth (approx. 500 m) differing with more than a factor of 2, partly caused by greater hydraulic gradients in Case 8. According to the particle trajectories, on the other hand, the path length and residence time is longer for a water particle in Case 8 than in Case 2, before it reaches one of the boundaries, i.e. a fracture zone.

Of all the nine cases utilized in the current study Case 3 and Case 5 are consequently distinguished, as these represent the extreme and, to each other, opposite groundwater conditions. Case 3 offers the most favourable conditions for a repository; small hydraulic gradients, homogeneous and low flow rates, long flow paths and residence time, and small groundwater recharge rates. Case 5 is the contradictory to this and is the worst of all cases.

According to Figure 4.6 all the cases put forward since the KBS 3-study, i.e. Case 4 to 9, implies greater groundwater flow rates at the potential repository. From the cases with variations of the fracture zone unit, Case 6 and Case 9 are the only ones with K(z)-functions that are not greater than for the KBS 3-cases (cf. Figure 4.2). For Case 9 the implementation of the "zone near" rock mass is, however, sufficient to create the higher flow rates, and for Case 6, with the constant hydraulic conductivity giving small K-values in the surficial parts of the fracture zones, the hydraulic conductivity at greater depth is apparently high enough to produce the higher flow rates. Almost the same explanation can, in principal, be given for the rock mass variants Case 8 and Case 7, respectively.

Although these differences between the model cases exist, it should also be pointed out that some results show good conformity e.g. the general groundwater flow pattern and the head

distribution. The groundwater flow is characterized by a flow inwards from the north and the south to a saddle point in the centre of the model domain. From the saddle point the groundwater is drained towards the regional fracture zones in the southwest and the northeast. All cases show the same mean groundwater head (approx. 54 m.a.s.l.) at the 500 m level and fairly small head range.

A potential case, not modelled here and which would have a rather large influence on the groundwater conditions of the site, is the possibility to treat the granite gneiss layers in the bedrock as individual discrete elements of great hydraulic conductivity in the same way as the local fracture zones have been treated. This implies that the granite gneiss layers are continuous and extended, a fact that at the present time can not be concluded even though some hydraulic data point in that direction, e.g. some low hydraulic heads in the granite gneiss indicate a connection with the western regional fracture zone.

5.1.2 Effect of anisotropic hydraulic properties

In general, the effect of anisotropy is disguised by the groundwater topography down to approximately 300 to 500 m depth. The effect of anisotropic hydraulic properties is expressed in different ways depending on which hydraulic parameter is considered and in which hydraulic unit the anisotropy exists.

The anisotropic rock mass in Fjällveden affect the groundwater flow pattern by skewing the isopotential curves to be more parallel with the main direction of anisotropy (NE direction), thus increasing the hydraulic gradient in the NW direction. Secondly, the groundwater flow rate is somewhat increased, primarily caused by the concurrence between the general hydraulic gradient and the main direction of anisotropy as these are oriented parallel. However, the implementation of the "zone near" rock mass, Case 8, have a much greater influence on the flow rates than the anisotropy itself.

The anisotropy of the fracture zones seems to have almost no effect on the flow rate but on the flow pattern, and the hydraulic gradients are slightly changed. This effect appears in the same way compared to the situation in the rock mass i.e. the gradient is decreased in the NE direction which in this case is perpendicular to the main direction of anisotropy. The configuration of the fracture zone network and its position in the isopotential head field may change the effect of anisotropy of the fracture zone.

Furthermore, the anisotropy of the rock mass as well as for the fracture zones induce the particle trajectories to slightly turn towards N. This is clearly demonstrated by comparing the Case 8 versus Case 9 and Case 1 versus Case 2, see Figure 4.7.

5.1.3 Effect of hydraulic contrast in the bedrock

It is obvious that the hydraulic gradient and the groundwater flow rates increase at greater depth when elements of greater hydraulic conductivity such as fracture zones or "zone near" rock mass are included in the model. In particular, the horisontal gradients are enhanced.

In cases like Case 3, where fracture zones are lacking and Case 6, where small K-values in the uppermost part of the fracture zones prevail, the vertical gradients become more emphasized relative to the horisontal ones and consequently the particle trajectories become more vertical.

5.1.4 Relevance of results

5.1.4.1 Groundwater recharge

The calculated groundwater recharge rates, ranging between 2 and 40 mm/year for the different cases, are within the interval expected from the current understanding of groundwater recharge in crystalline bedrock. However, the recharge rates reflect foremost the groundwater conditions in the uppermost part of

the bedrock and have little bearing upon the groundwater flow conditions at the potential repository level. For example, the Cases 5 and 6 show almost the same flow rates at 500 m depth but quite significant difference for the groundwater recharge, 39 mm/year and 2 mm/year, respectively.

In general, the varying hydraulic properties assigned to the bedrock in the different cases, lead to the same result; small recharge rates for the rock mass and great variations for the fracture zones. The corresponding situation is reflected for the size of the respective recharge areas.

Furthermore, the fracture zones have a predominant influence on the groundwater recharge when the conductivity contrast in the surficial bedrock is great.

5.1.4.2 Mass conservation of numerical solutions

Anisotropic hydraulic properties of the bedrock for the Fjällveden site is insignificant to the quality of numerical solutions, whereas great conductivity contrasts decrease the mass conservation. Three cases are distinguished; Case 3 giving the best mass conservation due to the lack of fracture zones and low hydraulic contrasts, and Case 5/Case 6 constituting the worst cases as the conductivity contrast and the hydraulic gradients are great.

5.2 Conclusions

The limited number of hydraulic conductivity data, especially for the fracture zones, have given rise to different conceptual model cases of which several can be regarded as being equally realistic. The calculated head distribution and flow rates for these model cases may differ very little, while their respective residence times in the bedrock may vary more significantly (2-3 times).

The continuity and extension of the highly conductive horizons of granite gneiss, and local fracture zones, along with their orientation relative to the hydraulic gradient, are decisive in determining the hydraulic conditions of the site. Anisotropic hydraulic properties on the other hand, are of secondary importance.

The groundwater recharge, as a factor of quality assurance of the model calculations at the 500 m level, is of limited use because it has little bearing on the conditions in the rock mass at depth. Here, the recharge is mainly determined by the hydraulic properties in the uppermost part of the fracture zones.

Finally, the restricted capacity of the computer has meant that certain simplifications have been necessary for discretisation of the conceptual model. For future calculations, this situation must be improved if more site specific modelling is to be utilized.

6. REFERENCES

Ahlbom, K., Carlsson, L., Carlsten, L-E., Duran, O., Larsson, N-Å. and Olsson, O., 1983a. Evaluation of the geological, geophysical and hydrogeological conditions at Fjällveden. SKB Technical Report 83-52, Stockholm.

Ahlbom, K., Carlsson, L. and Olsson, O., 1983b. Final disposal of spent nuclear fuel - geological, hydrogeological and geophysical methods for site characterization. SKB Technical Report 83-43, Stockholm.

Ahlbom, K., Carlsson, L., Gentzschein, B., Jämtlid, A., Olsson, O. and Tirén, S., 1983c. Evaluation of the geological, geophysical and hydrogeological conditions at Svartboberget. SKB Technical Report 83-55, Stockholm.

Carlsson, L., Winberg, A. and Grundfelt, B., 1983. Model calculations of the groundwater flow at Finnsjön, Fjällveden, Gideå and Kamlunge. SKB Technical Report 83-45, Stockholm.

Carlsson, L., Winberg, A. and Grundfelt, B., 1984. Hydraulic properties and modelling of potential repository sites in Swedish crystalline rock. IAEA - Seminar on the site investigation techniques and assessment methods for underground disposal of radioactive wastes. Sofia Bulgaria. IAEA-SR-104/15.

Dagan, G., 1979. Models of groundwater flow in statistically homogeneous formations. - Water Resources Research, Vol 15, No 1, Feb 1979, pp 47-63.

Dagan, G., 1981. Analysis of flow through heterogeneous random aquifers by the method of embedding matrix. 1. Steady flow.Water Resources Research, Vol 17, No 1, Feb 1981, pp 107-121.

Grundfelt, B., 1983. GWHRT - A finite element solution to the coupled ground water flow and heat transport problem in three dimensions. SKB Technical Report 83-51, Stockholm.

Neuzil, C-E. and Tracy, J.V., 1981. Flow through fractures. - Water Resources Research, Vol 17, No 1, Feb 1981, pp 191-199.

SKBF, 1983. Final storage of spent nuclear fuel - KBS 3, Stockholm.

Thunvik, R. and Braester, C., 1980. Hydrothermal conditions around a radioactive waste repository. SKB Technical Report 80-19, Stockholm.

APPENDIX I: Groundwater head distribution and flow field at the Fjällveden study site

The calculated groundwater head distribution is presented in one horisontal and four vertical cross-sections for Case 1 to 9, Figures 1 - 9.

The horisontal cross-section (upper right figure in Figure 1 - 9) is located at the level of the potential repository, i.e. 500m depth.

The location of the vertical cross-sections is illustrated in a horisontal view (upper left figure in Figure 1 - 9). The arrows in the vertical cross-sections are projections of the flux vectors onto the cross-sections. The length of the arrows are proportional to the logarithm of the darcy velocity. The direction of the third vector component is indicated by the type of arrow-head. A filled arrow-head indicates that the third component points up through the paper plane (towards the reader). The magnitude of the third component is, however not indicated.

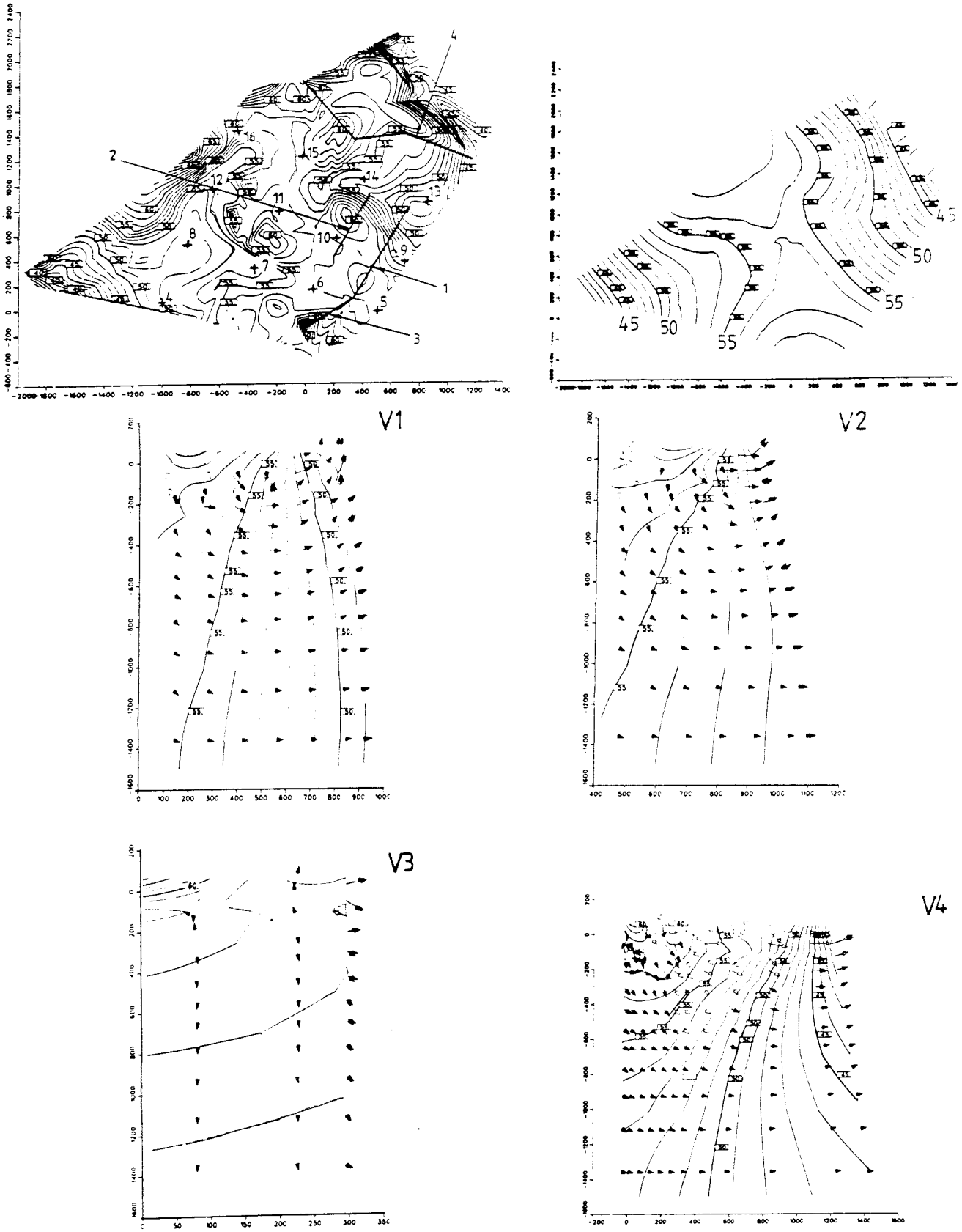

Figure 1 Isopotential curves for Case 1 in one horisontal cross-section at 500 m depth and four vertical cross-sections. Equidistance = 1 m.

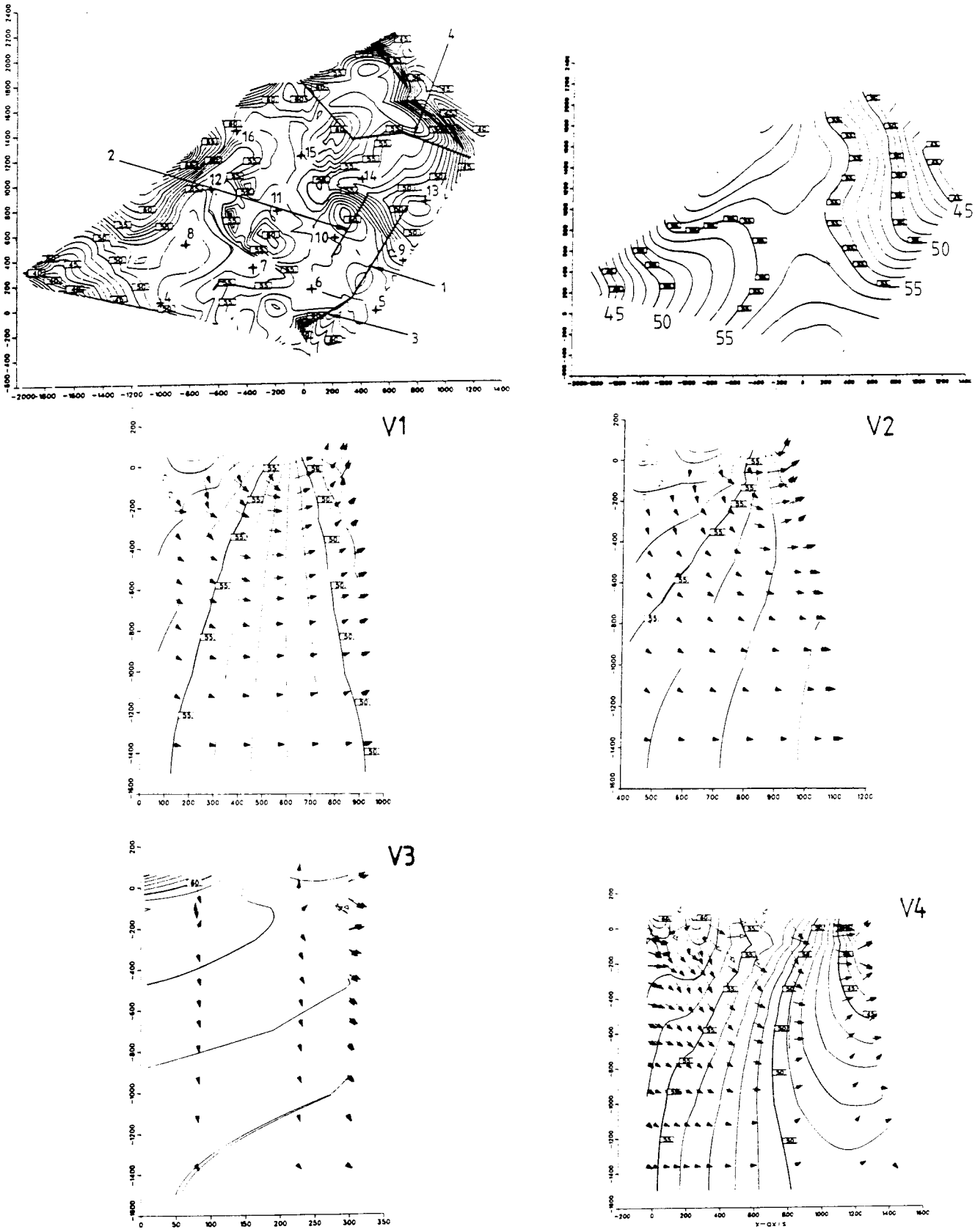

Figure 2 Isopotential curves for Case 2 in one horisontal cross-section at 500 m depth and four vertical cross-sections. Equidistance = 1 m.

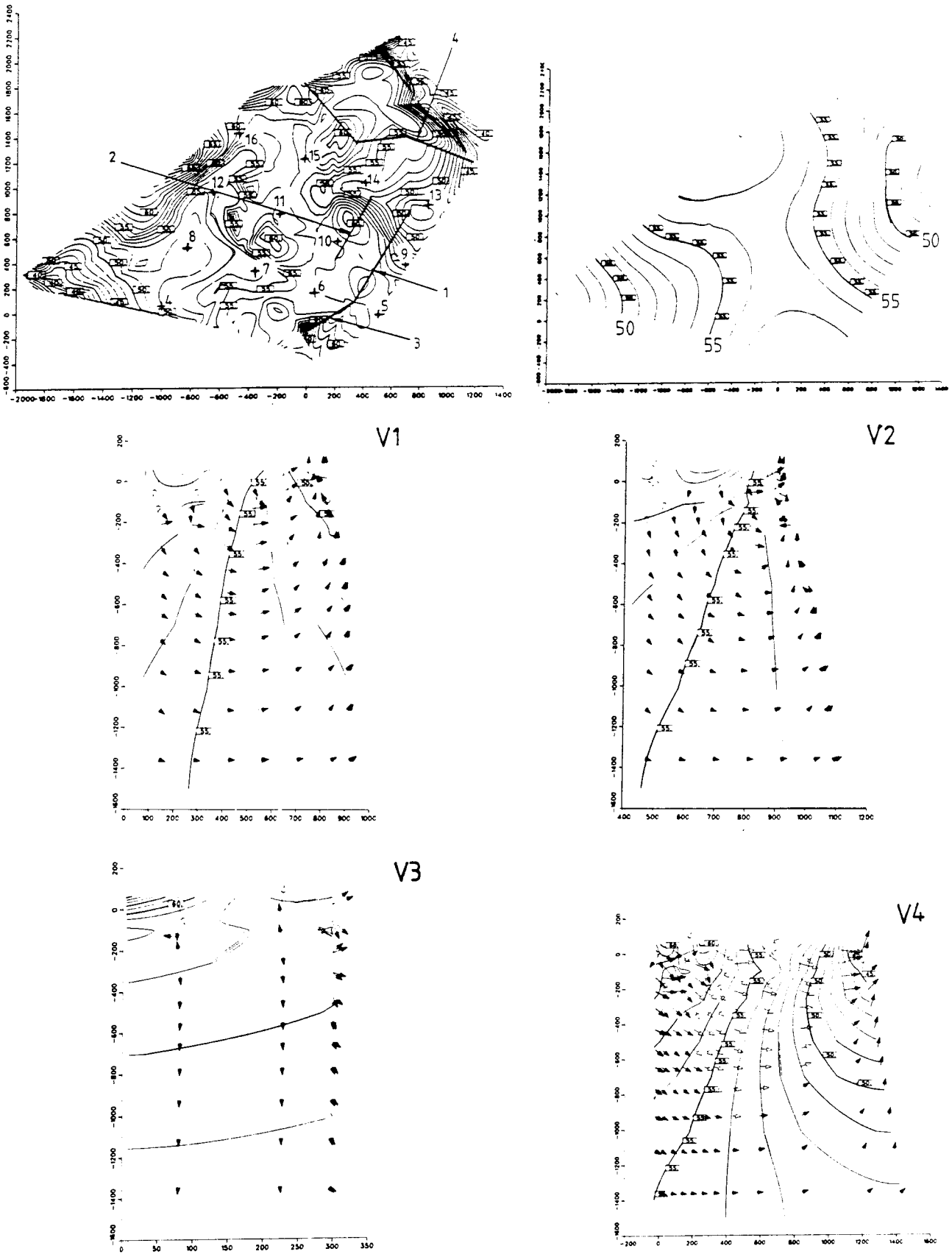

Figure 3 Isopotential curves for Case 3 in one horisontal cross-section at 500 m depth and four vertical cross-sections. Equidistance = 1 m.

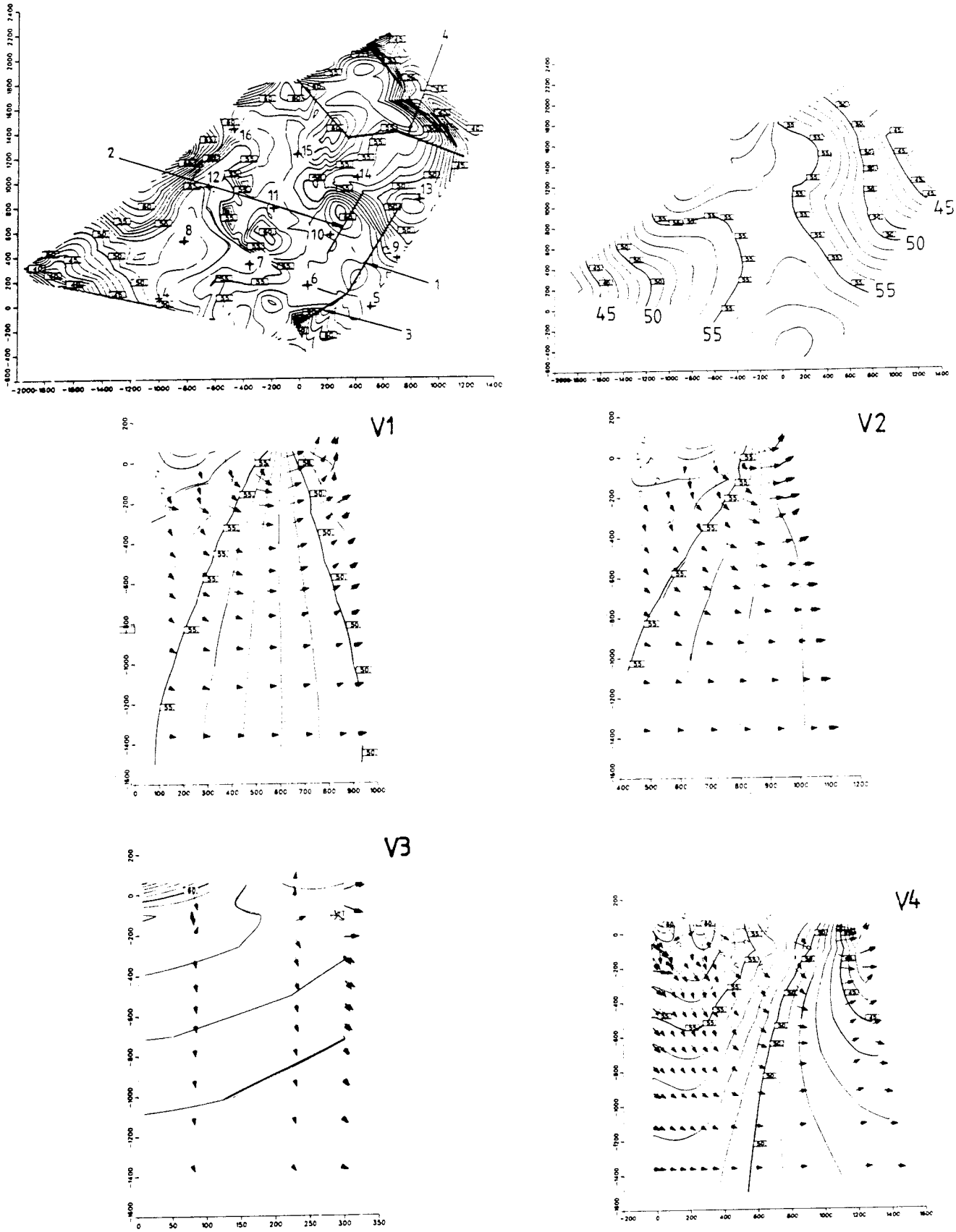

Figure 4 Isopotential curves for Case 4 in one horisontal cross-section at 500 m depth and four vertical cross-sections. Equidistance = 1 m.

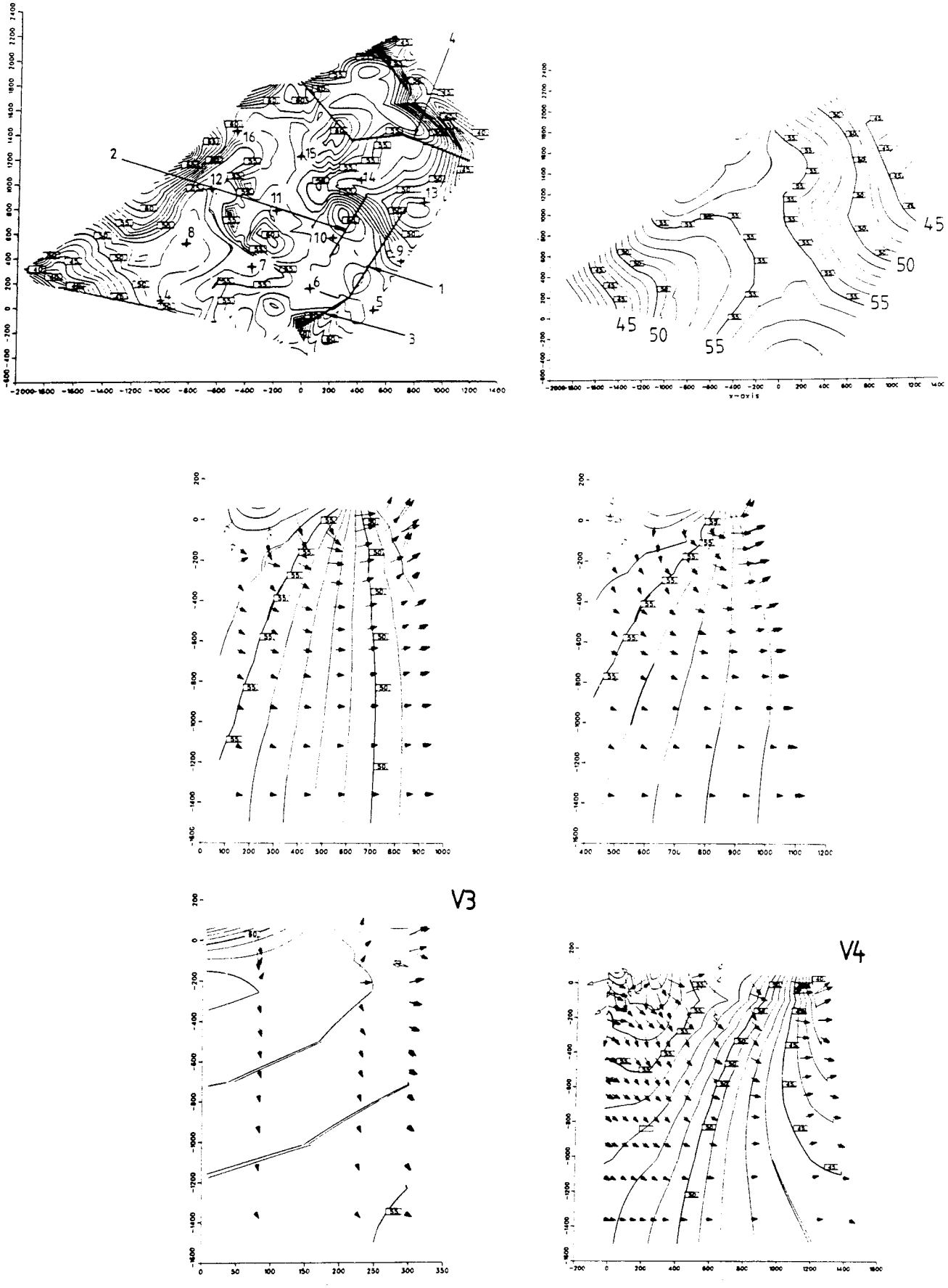

Figure 5 Isopotential curves for Case 5 in one horisontal cross-section at 500 m depth and four vertical cross-sections. Equidistance = 1 m.

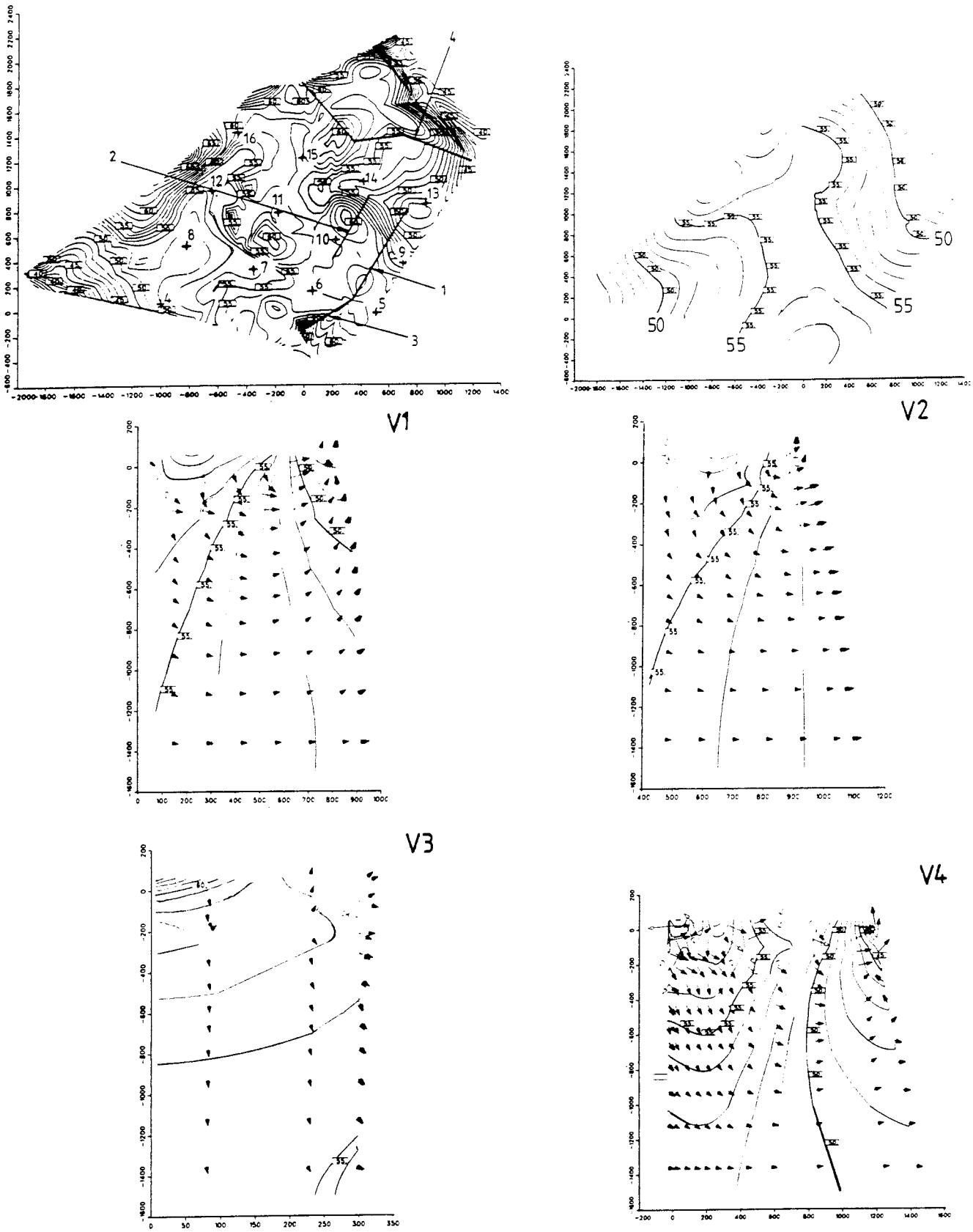

Figure 6 Isopotential curves for Case 6 in one horisontal cross-section at 500 m depth and four vertical cross-sections. Equidistance = 1 m.

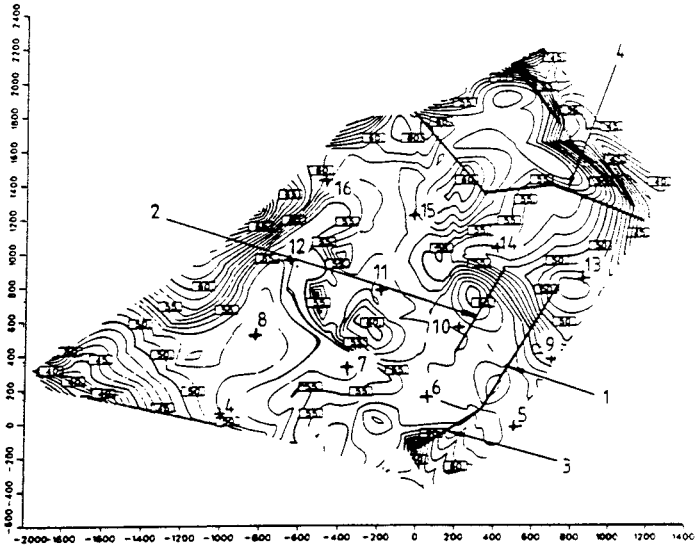

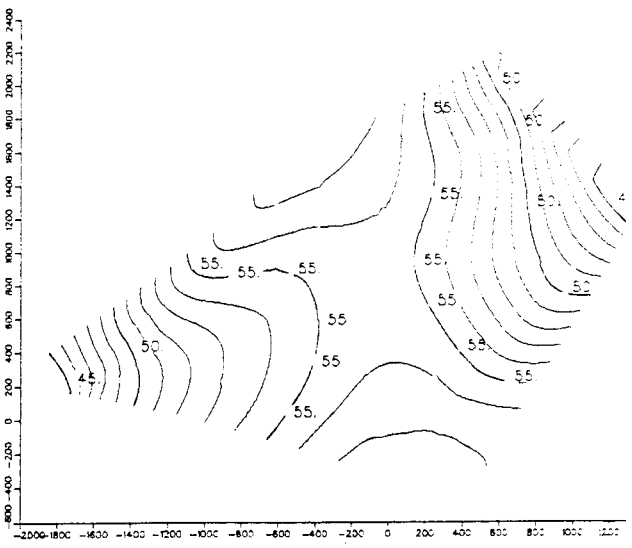

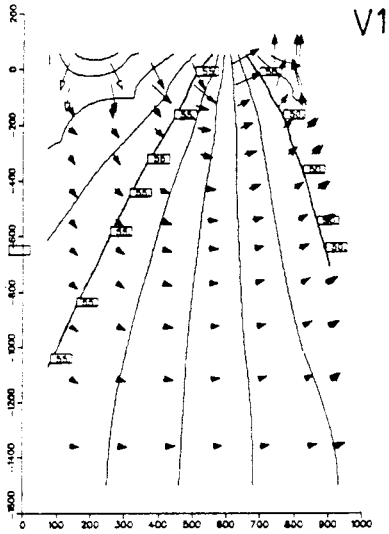

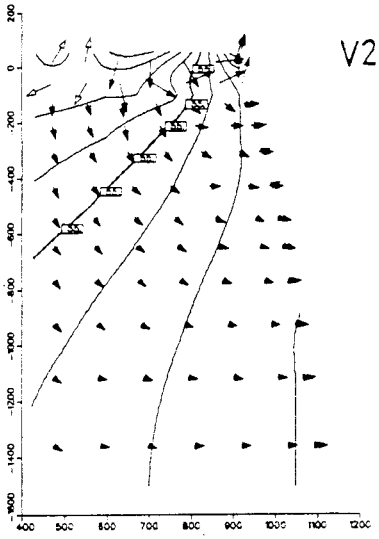

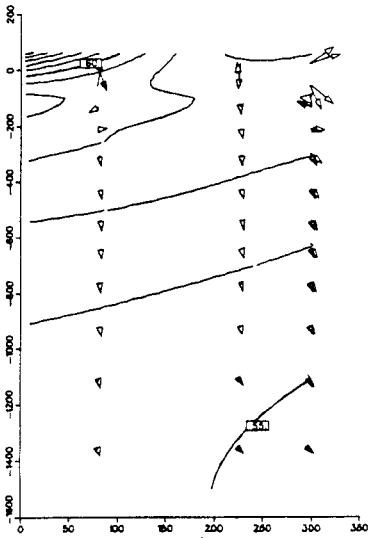

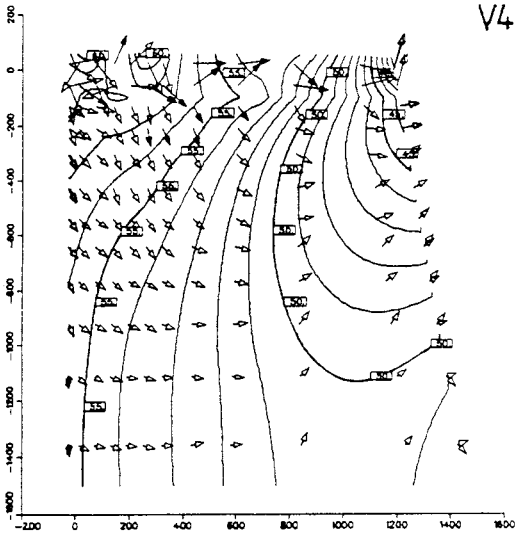

Figure 7 Isopotential curves for Case 7 in one horisontal cross-section at 500 m depth and four vertical cross-sections. Equidistance = 1 m.

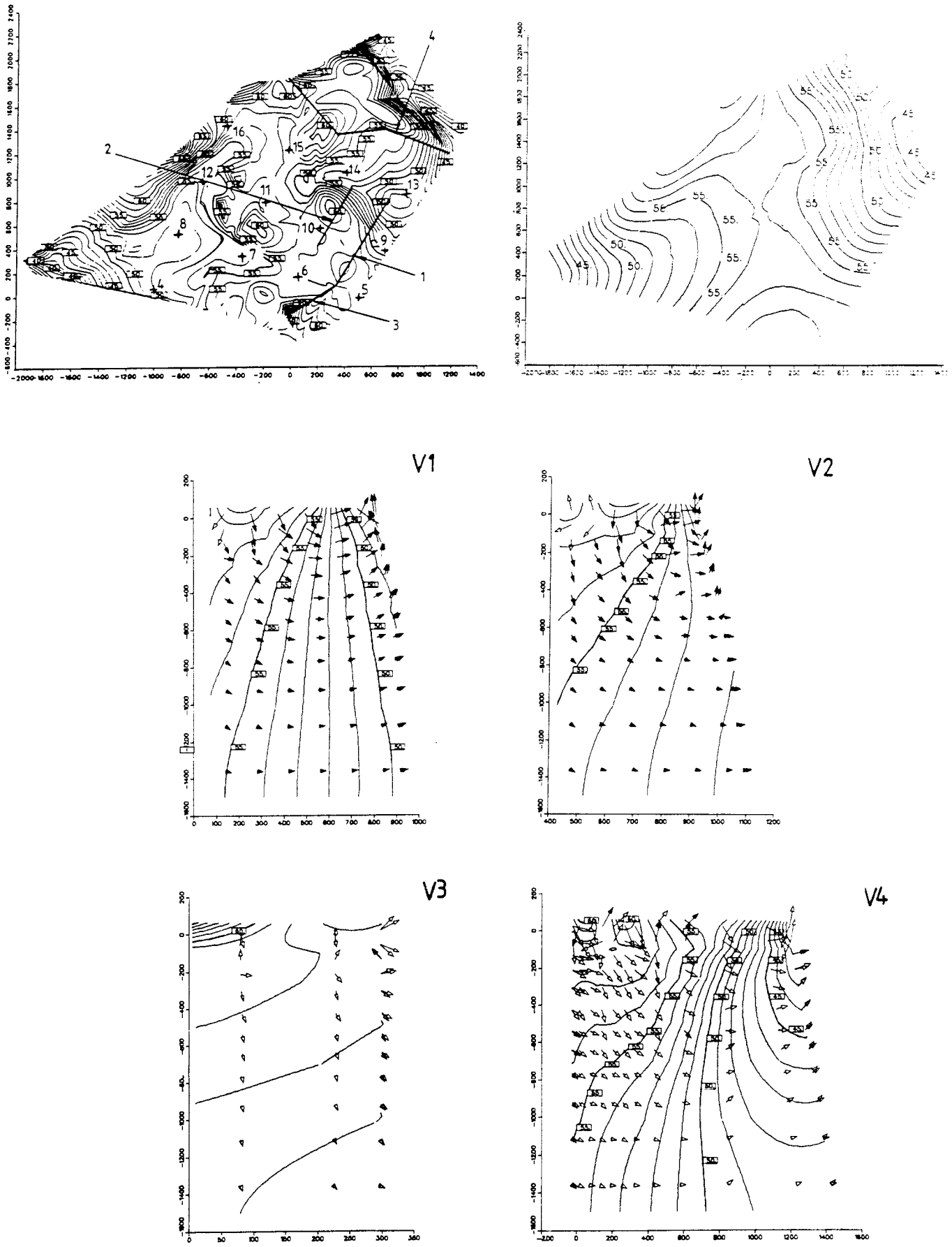

Figure 8 Isopotential curves for Case 8 in one horisontal cross-section at 500 m depth and four vertical cross-sections. Equidistance = 1 m.

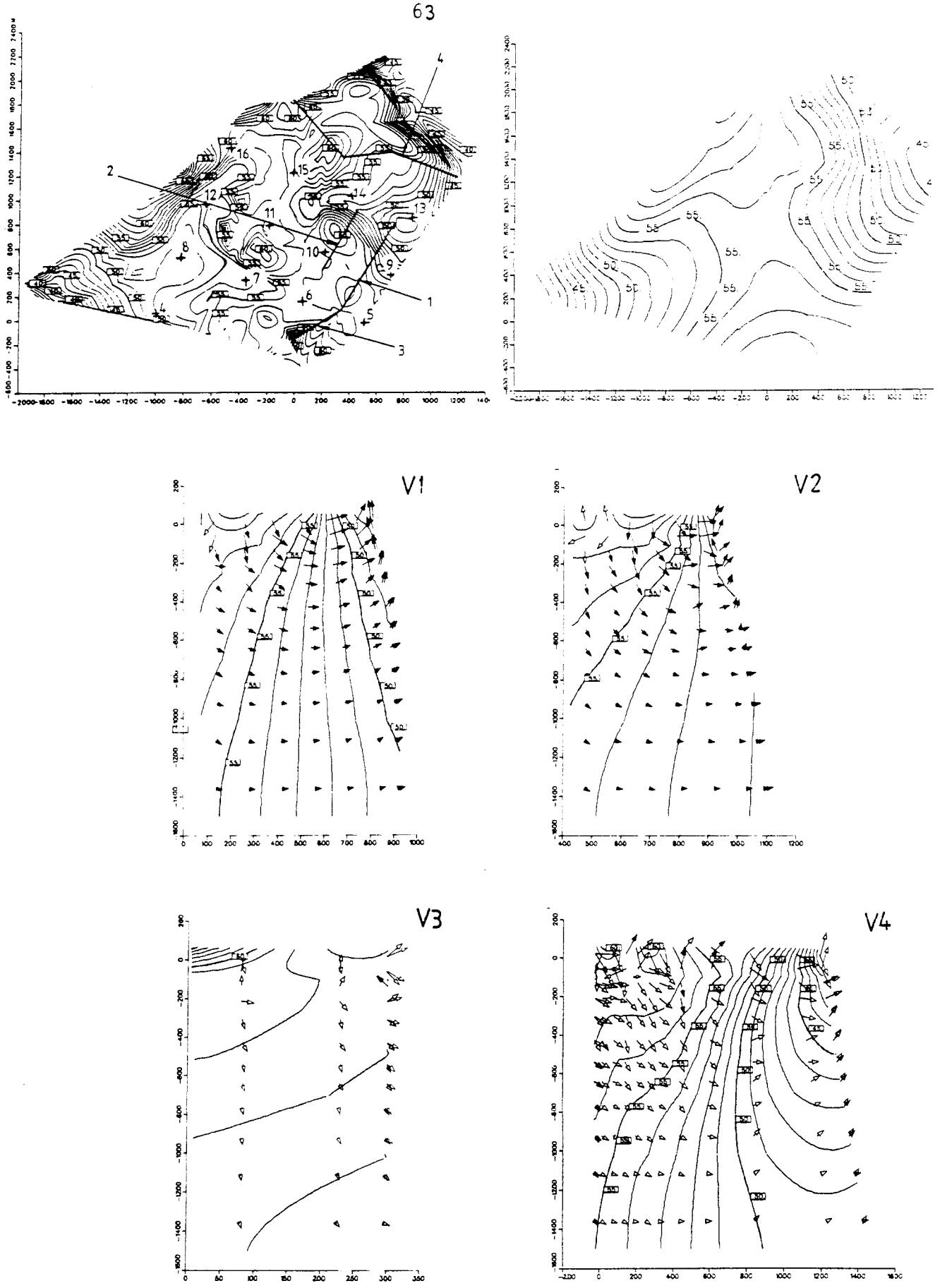

Figure 9 Isopotential curves for Case 9 in one horisontal cross-section at 500 m depth and four vertical cross-sections. Equidistance = 1 m.

List of SKB reports

Annual Reports

1977–78
TR 121
KBS Technical Reports 1 – 120.
Summaries. Stockholm, May 1979.

1979
TR 79–28
The KBS Annual Report 1979.
KBS Technical Reports 79-01 – 79-27.
Summaries. Stockholm, March 1980.

1980
TR 80–26
The KBS Annual Report 1980.
KBS Technical Reports 80-01 – 80-25.
Summaries. Stockholm, March 1981.

1981
TR 81–17
The KBS Annual Report 1981.
KBS Technical Reports 81-01 – 81-16.
Summaries. Stockholm, April 1982.

1982
TR 82–28
The KBS Annual Report 1982.
KBS Technical Reports 82-01 – 82-27.
Summaries. Stockholm, July 1983.

1983
TR 83–77
The KBS Annual Report 1983.
KBS Technical Reports 83-01 – 83-76
Summaries. Stockholm, June 1984.

1984
TR 85–01
Annual Research and Development Report 1984
Including Summaries of Technical Reports Issued during 1984. (Technical Reports 84-01–84-19)
Stockholm June 1985.

1985
TR 85-20
Annual Research and Development Report 1985
Including Summaries of Technical Reports Issued during 1985. (Technical Reports 85-01-85-19)
Stockholm May 1986.

1986
TR 86-31
SKB Annual Report 1986
Including Summaries of Technical Reports Issued during 1986
Stockholm, May 1987

1987
TR 87-33
SKB Annual Report 1987
Including Summaries of Technical Reports Issued during 1987
Stockholm, May 1988

Technical Reports

1988

TR 88-01
Preliminary investigations of deep ground water microbiology in Swedish granitic rocks
Karsten Pedersen
University of Göteborg
December 1987

TR 88-02
Migration of the fission products strontium, technetium, iodine, cesium and the actinides neptunium, plutonium, americium in granitic rock
Thomas Ittner[1], Börje Torstenfelt[1], Bert Allard[2]
[1]Chalmers University of Technology
[2]University of Linköping
January 1988

TR 88-03
Flow and solute transport in a single fracture A two-dimensional statistical model
Luis Moreno[1], Yvonne Tsang[2], Chin Fu Tsang[2], Ivars Neretnieks[1]
[1]Royal Institute of Technology, Stockholm, Sweden
[2]Lawrence Berkeley Laboratory, Berkeley, CA, USA
January 1988

TR 88-04
Ion binding by humic and fulvic acids: A computational procedure based on functional site heterogeneity and the physical chemistry of polyelectrolyte solutions
J A Marinsky, M M Reddy, J Ephraim, A Mathuthu
US Geological Survey, Lakewood, CA, USA
Linköping University, Linköping
State University of New York at Buffalo, Buffalo, NY, US/
April 1987

TR 88-05
Description of geophysical data on the SKB database GEOTAB
Stefan Sehlstedt
Swedish Geological Co, Luleå
February 1988

TR 88-06
Description of geological data in SKBs database GEOTAB
Tomas Stark
Swedish Geological Co, Luleå
April 1988

TR 88-07
Tectonic studies in the Lansjärv region
Herbert Henkel
Swedish Geological Survey, Uppsala
October 1987

TR 88-08
Diffusion in the matrix of granitic rock. Field test in the Stripa mine. Final report.
Lars Birgersson, Ivars Neretnieks
Royal Institute of Technology, Stockholm
April 1988

TR 88-09
The kinetics of pitting corrosion of carbon steel. Progress report to June 1987
G P Marsh, K J Taylor, Z Sooi
Materials Development Division
Harwell Laboratory
February 1988

TR 88-10
GWHRT – A flow model for coupled groundwater and heat flow
Version 1.0
Roger Thunvik[1], Carol Braester[2]
[1] Royal Institute of Technology, Stockholm
[2] Israel Institute of Technology, Haifa
April 1988